



# Volcanic CO<sub>2</sub> seep geochemistry and use in understanding ocean acidification

A. Aiuppa · J. M. Hall-Spencer · M. Milazzo · G. Turco · S. Caliro · R. Di Napoli

Received: 8 March 2020 / Accepted: 24 November 2020  
© The Author(s) 2020

**Abstract** Ocean acidification is one of the most dramatic effects of the massive atmospheric release of anthropogenic carbon dioxide (CO<sub>2</sub>) that has occurred since the Industrial Revolution, although its effects on marine ecosystems are not well understood. Submarine volcanic hydrothermal fields have geochemical conditions that provide opportunities to characterise the effects of elevated levels of seawater CO<sub>2</sub> on marine life in the field. Here, we review the geochemical aspects of shallow marine CO<sub>2</sub>-rich seeps worldwide, focusing on both gas composition

and water chemistry. We then describe the geochemical effects of volcanic CO<sub>2</sub> seepage on the overlying seawater column. We also present new geochemical data and the first synthesis of marine biological community changes from one of the best-studied marine CO<sub>2</sub> seep sites in the world (off Vulcano Island, Sicily). In areas of intense bubbling, extremely high levels of pCO<sub>2</sub> (> 10,000 μatm) result in low seawater pH (< 6) and undersaturation of aragonite and calcite in an area devoid of calcified organisms such as shelled molluscs and hard corals. Around 100–400 m away from the Vulcano seeps the geochemistry of the seawater becomes analogous to future ocean acidification conditions with dissolved carbon dioxide levels falling from 900 to 420 μatm as seawater pH rises from 7.6 to 8.0. Calcified species such as coralline algae and sea urchins fare increasingly well as sessile communities shift from domination by a few resilient species (such as uncalcified algae and polychaetes) to a diverse and complex community (including abundant calcified algae and sea urchins) as the seawater returns to ambient levels of CO<sub>2</sub>. Laboratory advances in our understanding of species sensitivity to high CO<sub>2</sub> and low pH seawater, reveal how marine organisms react to simulated ocean acidification conditions (e.g., using energetic trade-offs for calcification, reproduction, growth and survival). Research at volcanic marine seeps, such as those off Vulcano, highlight consistent ecosystem responses to rising levels of seawater CO<sub>2</sub>, with the simplification of food webs, losses in functional

---

Responsible Editor: Kelman Wieder

---

**Supplementary Information** The online version of this article (<https://doi.org/10.1007/s10533-020-00737-9>) contains supplementary material, which is available to authorized users.

---

A. Aiuppa (✉) · M. Milazzo · G. Turco · R. Di Napoli  
Dipartimento di Scienze della Terra e del Mare,  
Università di Palermo, Palermo, Italy  
e-mail: [alessandro.aiuppa@unipa.it](mailto:alessandro.aiuppa@unipa.it)

J. M. Hall-Spencer  
School of Biological and Marine Sciences, University of  
Plymouth, Plymouth, UK

J. M. Hall-Spencer  
Shimoda Marine Research Center, University of Tsukuba,  
Tsukuba, Japan

S. Caliro  
Istituto Nazionale di Geofisica e Vulcanologia,  
Osservatorio Vesuviano, Napoli, Italy

diversity and reduced provisioning of goods and services for humans.

**Keywords** Calcifying species · Ecosystem effects · Natural analogues · Submarine hydrothermalism

## Introduction

Rising atmospheric carbon dioxide levels, from fossil fuel combustion and other human activities, are increasing seawater CO<sub>2</sub> levels and reducing the carbonate saturation of estuarine, coastal, and surface open-ocean waters (IPCC 2019; Doney et al. 2020). This has globally expanded the volume of seawater that is corrosive to carbonate (Tittensor et al. 2009) and first came to world attention when ocean acidification caused mass oyster spat mortality, threatening a \$270 million/year aquaculture industry in Washington State, USA (Ekstrom et al. 2015). Field manipulations of seawater CO<sub>2</sub> have shown that ocean acidification causes carbonate saturation state to fall below levels suitable for globally important coral reefs (Albright et al. 2018) and laboratory studies show that acidification can reduce the nutritional value of seafood as it lowers caloric content and levels of protein, lipid and carbohydrate (Lemasson et al. 2019). Thus acidification puts at risk many of the valuable ecosystem services that the ocean provides to society, such as fisheries, aquaculture, and shoreline protection (Hall-Spencer and Harvey 2019; Doney et al. 2020).

Although the chemistry of ocean acidification (OA) is well understood, there is uncertainty about the ecosystem effects of these changes. Laboratory experiments show that OA may affect all marine life, for example through changes in gene expression, physiology, reproduction and behaviour (IPCC 2019). However, it is difficult to scale-up from these results as most laboratory studies address only the effect of one or two parameters on a single organism, since multiparameter studies using multiple species are logistically challenging (Riebesell and Gattuso 2015). In the past 10 years, work using natural gradients in pCO<sub>2</sub> has shown the long-term effects of OA on ecosystem properties, functions and services. Many studies have been conducted at shallow submarine hydrothermal vents around active volcanoes (here referred to as hydrothermal CO<sub>2</sub> seeps), where large

amounts of CO<sub>2</sub> are injected into seawater (Fig. 1; Hall-Spencer et al. 2008). These shallow (< 200 m) hydrothermal CO<sub>2</sub> seeps (Tarasov et al. 2005; Dando 2010; González-Delgado and Hernández 2018) provide natural analogues to study the impact of OA on ecosystems. Volcanic CO<sub>2</sub> seeps also help further our understanding of the subsurface hydrothermal structure of coastal volcanoes, where a significant fraction of the hydrothermal output can occur offshore (Italiano and Nuccio 1991; Pichler et al. 1999a; Di Napoli et al. 2016). From a geochemical viewpoint, these sites allow studies of the dispersion patterns of seep-carried CO<sub>2</sub> and water-soluble chemicals in seawater (Boatta et al. 2013; Price and Giovannelli 2017; Pichler et al. 2019).

Here, we review the geochemistry of hydrothermal CO<sub>2</sub> seeps and use one of the best-known sites (off Vulcano Island, Sicily) as a case study. This expands on (and complements) recent excellent reviews on the topic (Dando 2010; Price and Giovannelli 2017; González-Delgado and Hernández 2018) by (i) combining available gas and aqueous compositional data for 56 seeps to illustrate quantitatively (in a set of key plots) the *processes* that govern and control their chemistry; (ii) providing a combination of new geochemical and biological data from Vulcano, including a demonstration on the potential of novel geochemical techniques to study seeps; (iii) presenting a novel and systematic analysis of biological data on how the abundances of higher taxa change at Vulcano in response to OA. Doing so, we present recent advances in biological research when using volcanic



**Fig. 1** Example of vent forming sites/fields in shallow waters from Baia di Levante, Vulcano Island (Italy) Photo credit: Nicolas Floc'h

CO<sub>2</sub> seeps to assess the potential effects of OA and discuss ecosystem responses, describing which organisms survive well in acidified conditions and which do not. We end by presenting future research paths to be explored.

## Marine CO<sub>2</sub> seeps

### Types of submarine CO<sub>2</sub> seeps

Carbon dioxide-rich fluid venting on the seafloor is a common geological process. The discovery of vigorous fluid venting at Middle-Oceanic Ridges (MOR) in the 1970s boosted a plethora of studies on both the chemical properties of these ‘black and white smokers’ and on the biological communities living therein (Von Damm 1990; Tunncliffe 1991). Gas venting at MORs is now recognised as a primary pathway of volatile (CO<sub>2</sub>, noble gases) exchange from the Earth’s mantle to the hydrosphere and atmosphere (Marty et al. 2013). MOR fluids have also been intensively studied because they transport the key chemical ingredients for life (e.g., reduced compounds of the elements C, O, N, S), and are thus potential candidate sites for the origin of life on our planet (Baross and Hoffman 1985). Recent focus has been on these fluids as sources of Fe, Mn, Zn and other micronutrients to the ocean, and on their role in the formation of massive sulphide deposits (Hannington et al. 2005, 2011). However, MOR seeps, alongside with their equivalent in active subduction zones (see de Ronde and Stucker 2015 for a review), typically occur several km deep in the ocean, far from coasts and well below the euphotic zone. They have low biological diversity and a fauna that relies on carbon fixation by chemosynthesis (Tunncliffe 1991). Consequently, these deep vents are unsuitable proxies for studying the effects of OA on coastal marine biological communities (Dando 2010; González-Delgado and Hernández 2018).

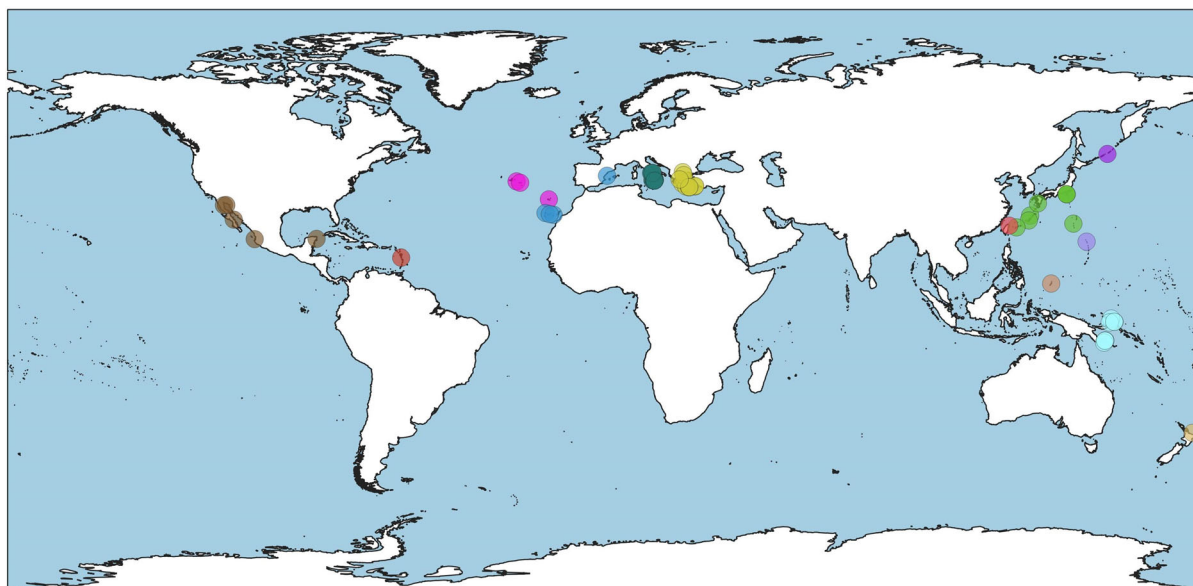
Here, we focus on CO<sub>2</sub> seeps in shallow (< 200 m) waters which have marine communities that are more diverse and are not dominated by chemosynthetic organisms (Tarasov et al. 2005; Dando 2010; González-Delgado and Hernández 2018). Shallow high CO<sub>2</sub> areas can be produced by a variety of processes, including (González-Delgado and Hernández 2018): (i) karstic groundwater inflow (e.g., Yucatan Peninsula, Gulf of Mexico; Crook et al. 2016); (ii) rainwater

and meteoric water inflow into small confined seawater basins, combined with high rate of respiration by living organisms (e.g., Rocas Islands of Palau Oceania; Shamberger et al. 2014); (iii) upwelling of seawater rich in inorganic C (e.g., Kiel Bay in the Baltic Sea; Thomsen et al. 2010); and (iv) discharge at the seafloor of CO<sub>2</sub>-rich volcanic-hydrothermal fluids. This latter process can lead to both seawater acidification and to (small and confined) temperature increases (Di Napoli et al. 2016). It is on category (iv) above that we focus on below.

### Global occurrence of shallow hydrothermal CO<sub>2</sub> seeps, and their geological significance

Submarine CO<sub>2</sub> seeps are likely to exist around any active coastal or island volcano, or on top of shallow seamounts (Price and Giovannelli 2017). The relatively small number of reports reflects technical challenges in locating and exploring them. Of the 70 reported shallow volcano-related seep locations (Price and Giovannelli 2017), we have identified 56 (Fig. 2) for which chemical and biological information exists (see Table S1, Fig. 2 caption for data provenance). The geographical distribution of these sites, illustrated in the map of Fig. 2, shows clusters in specific areas (e.g., the Mediterranean, Japan-southeast Asia and US). In the field, volcano-related seeps occur as single, gas-rich vents bubbling through the overlying seawater column or, more frequently, as cluster of vents forming sites/fields tens to several hundred square meters in size (Fig. 1). In addition to focused vent emissions, so called “diffuse vents” have also commonly been reported.

Throughout this review, we refer to these volcano-related seeps as hydrothermal CO<sub>2</sub> seeps because, geologically speaking, they are due to the interaction between fluids rising from volcanic hydrothermal systems and seawater (Fig. 3). These dynamic environments exhibit large spatial and temporal variations in aqueous fluid and gas chemistry (as well as in their discharge rates), owing to the complex interplay of factors such as local hydrothermal/geological setting, temperature, pressure, pH, fluid-rock interaction extent, and host rock geology. Broadly speaking, submarine hydrothermal systems form as seawater-derived (or meteoric-derived) waters percolate through permeable volcanic rocks, and become heated by dissolving magmatic volatiles rising from deep-



### Locations of the shallow water vent sites

- |                               |                    |                                |                    |               |
|-------------------------------|--------------------|--------------------------------|--------------------|---------------|
| ● Dominica (Les Antilles) (1) | ● Japan (24-31)    | ● Northern Mariana Island (38) | ● Portugal (48-50) | ● Taiwan (56) |
| ● Greece (2-12)               | ● Mexico (32-36)   | ● Palau (39)                   | ● Russia (51)      |               |
| ● Italy (13-23)               | ● New Zealand (37) | ● Papua New Guinea (40-47)     | ● Spain (52-55)    |               |

**Fig. 2** Locations of shallow water vent sites. The number in brackets refers to the ID code of each location, see Table S1 for further details. (Color figure online)

seated magma storage zones (Price and Giovannelli 2017) (Fig. 3). As such, hydrothermal systems act as chemical filters, scavenging water-soluble magmatic volatiles to hydrothermal solutions (as  $\text{Cl}^-$ ,  $\text{SO}_4^{2-}$ ,  $\text{HS}^-$ , etc.) and minerals (sulphides, silicates), and converting magmatic volatiles ( $\text{CO}_2$ ,  $\text{CO}$ ,  $\text{SO}_2$ ) into hydrothermal gases ( $\text{CH}_4$ ,  $\text{H}_2\text{S}$ ) via equilibrium gas–water–rock reactions at reservoir P–T–redox conditions (Giggenbach 1980, 1997; Chiodini and Marini 1998; Fischer and Chiodini 2015) (Fig. 3). At reservoir conditions, hydrothermal fluids are typically two-phase (liquid + reservoir gas) but liquid-dominated (Giggenbach 1997). This aqueous phase is typically a Na–K–Cl brine (Price and Giovannelli 2017) enriched in alkalis and Ca due to extensive leaching of the host rocks (see “Aqueous fluid chemistry” section), and boils to steam as it decompresses upon ascent through geological discontinuities (faults or permeability barriers) (Chiodini and Marini 1998). Upon approach to the near-seafloor, steam and brine mix with cool infiltrating seawater, enriching the residual steam

phase in  $\text{CO}_2$  (that has limited water solubility at hydrothermal conditions) and the residual liquid in seawater components (Mg, Na, K, Cl). Finally, upon discharge, the  $\text{CO}_2$ -rich gases bubble through, and partially dissolve into, seawater, increasing seawater  $\text{CO}_2$  partial pressure ( $\text{pCO}_2$ ) and Dissolved Inorganic Carbon (DIC), and lowering surrounding seawater pH. The C-rich plumes that develop in the water column range considerably in size, as they depend on vent/site/field geometry, fluid (liquid + gas) output rate, temperature (controlling buoyancy) and hydrodynamic parameters (e.g., seawater current) (Fig. 3). The gradients in seawater carbonate chemistry create environments that allow studies into the impact of OA on local ecosystems.

#### The Baia di Levante hydrothermal $\text{CO}_2$ vents

One  $\text{CO}_2$  seep intensively studied by OA research is the Baia di Levante site in Vulcano Island (Aeolian Islands, Sicily) (Boatta et al. 2013). This small bay,

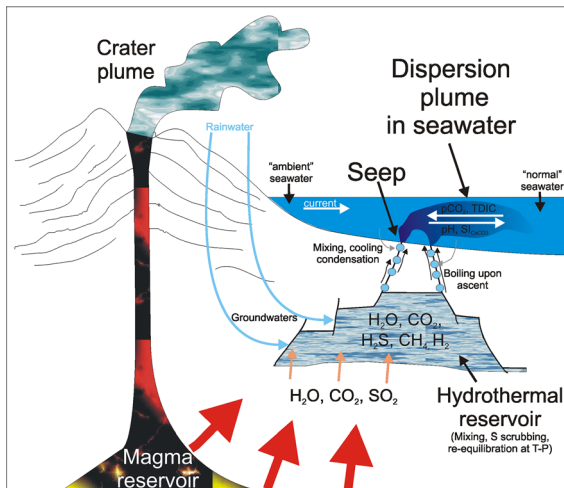


**Fig. 3** Geological sketch (not to scale) illustrating the mechanisms governing origin and chemistry of  $\text{CO}_2$  hydrothermal seeps at a coastal/insular volcano (see discussion). Red and orange arrows refer to magmatic volatile release from magma and injection into the hydrothermal system, respectively. Light blue and grey arrows identify meteoric recharge and entraining seawater, respectively. The white arrows indicate increasing DIC/ $\text{pCO}_2$  and Saturation Index (SI)/pH in the seawater column. (Color figure online)

located on the north-eastern margin of the island (Fig. 4), is well known since antiquity for the presence of numerous  $\text{CO}_2$ -rich submarine fumaroles discharging on the seafloor at less than a few meters depth

(Italiano and Nuccio 1991; Italiano et al. 1984, 1994; Chiodini et al. 1993, 1995; Capaccioni et al. 2001; Italiano 2009). These fumaroles have compositions typical of hydrothermal steam samples ( $\sim 90$  mol%  $\text{H}_2\text{O}$ ;  $\sim 90$  mol%  $\text{CO}_2$  and 2 mol%  $\text{H}_2\text{S}$  on a dry gas basis; see “Chemical impact of hydrothermal  $\text{CO}_2$  venting on the seawater column” section), and are thus interpreted as vapours deriving from boiling of hydrothermal brines rising from a shallow geothermal aquifer, identified during exploratory drilling (in 1951–1957) in the Levante Bay beach area (Sommaruga 1984). The geothermal aquifer itself is thought to be fed by magma-derived fluids similar to those feeding the La Fossa Crater further to the south (Chiodini et al. 1993, 1995; Paonita et al. 2013), although some authors (e.g., Tedesco 1995) have argued for a link with the Vulcanello magmatic system instead (Fig. 4). The dissolution of rising  $\text{H}_2\text{S}$ -rich hydrothermal steam leads to reduced (Eh as low as  $-150$  mV) and  $\text{H}_2\text{S}$ -rich ( $166$ – $273$   $\mu\text{mol/kg}$ ) conditions close to shore at the main submarine vents in the bay (Sedwick and Stüben 1996; Boatta et al. 2013). The high  $\text{CO}_2$  output ( $\sim 3.6$  ton/day of  $\text{CO}_2$  are discharged by submarine fumaroles into the bay; Inguaggiato et al. 2012) results in acidic conditions (pH as low as  $\sim 6.5$ ; see below) close to the vents. Also,  $\text{CO}_2$  seeping at the seafloor leads to strong pH gradients throughout the entire bay, with pH ranging

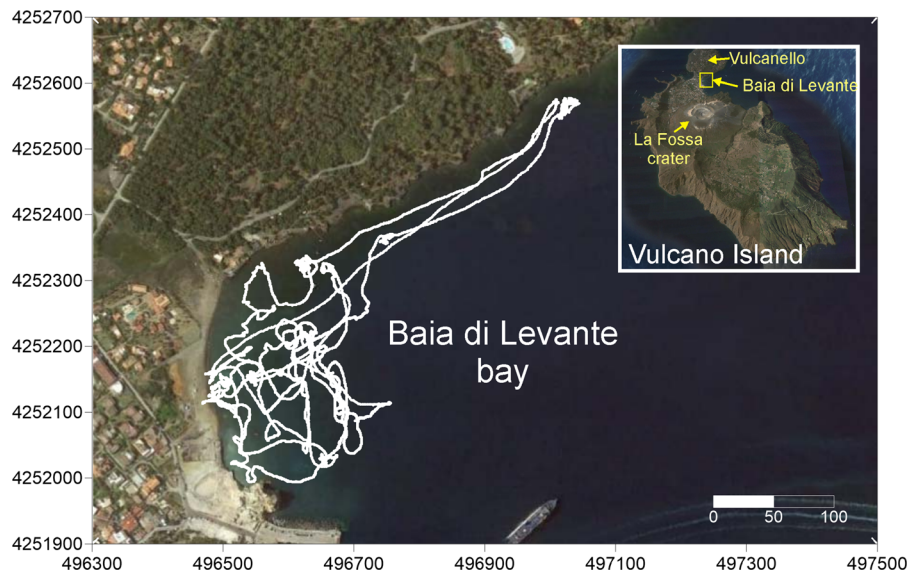


**Fig. 4** The Baia di Levante Bay area on Vulcano island (top right inset). The white line identifies the track of the  $\text{pCO}_2$  measurement profile along the bay

from vent-related values (< 6) to normal seawater levels (8.1) in a few hundreds meters from the vent (see below). These conditions make the Baia di Levante a natural laboratory to characterise the impact of OA on marine ecosystems (Boatta et al. 2013).

## Chemistry of hydrothermal CO<sub>2</sub> seeps

### Gas geochemistry

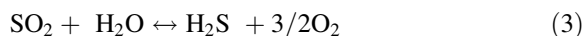
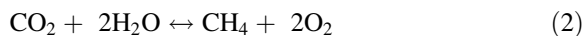
Collecting total (gas + steam) seep samples is technically difficult in the field. The steam fraction of shallow submarine hydrothermal CO<sub>2</sub> seeps is in fact rarely measured (gas analyses are typically expressed on a dry basis, as mol%, ppmv, mmol/mol or μmol/mol of the dry free gas; see Table S2). However, the few data available (e.g., Chiodini et al. 1995) confirm that, similar to their subaerial equivalents (Giggenbach 1980; Chiodini and Marini 1998), submarine hydrothermal seeps are mainly dominated by steam.

On a dry basis, shallow hydrothermal seeps are dominated by CO<sub>2</sub>. Table S2 lists some free gas analyses taken at several CO<sub>2</sub> seeps worldwide (see Fig. 2 for their location). Our compilation is not exhaustive of all shallow submarine vents studied, but includes gas compositional data for all (at least, to the best of our knowledge) those seeps studied so far for their ecology and biology. As such, our compilation is based upon (and is an updated version of) previous cataloguing efforts (Tarasov et al. 2005; Dando 2010; Price and Giovannelli 2017; Gonzáles-Delgado and Hernández 2018; Global CCS institute 2018).

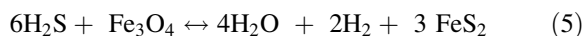
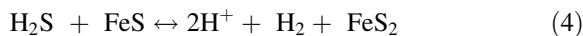
In our inventory (n = 207 gas analyses), the mean CO<sub>2</sub> content is 87 ± 20.7 vol%. The range is wide, from 0.4 to 99.6 vol%, but only 14 out of the 207 gas analyses have CO<sub>2</sub> < 50%. Where this occurs, the reduced CO<sub>2</sub> contents are systemically associated with increasing N<sub>2</sub> and O<sub>2</sub> contents (Table S2). Thus, the large spread of CO<sub>2</sub> contents in our compilation mostly reflects variable extents of magmatic gas dilution by air components (Fig. 5a), either deep in the hydrothermal reservoir or (more likely) during steam migration toward the surface and/or upon discharge on the seafloor. Shallow dilution by air is likely implicated by samples with N<sub>2</sub>/O<sub>2</sub> of ~ 3.7 (the typical air ratio), while deeper (reservoir) air entrainment is perhaps more likely for N<sub>2</sub>-rich samples

with N<sub>2</sub>/O<sub>2</sub> ratios > > 3.7. In hydrothermal reservoirs, atmospheric oxygen is consumed by redox reactions between fluids and host rocks (Giggenbach 1987) and, when this happens, the resulting surface gas emissions typically depart from the pure CO<sub>2</sub>-air mixing line (green solid line of Fig. 5). In addition to atmospheric O<sub>2</sub> consumption, magmatic N<sub>2</sub> feeding to the source hydrothermal systems (Pichler et al. 1999a) can also justify the N<sub>2</sub>-enriched samples. Figure 5a also shows that the Baia di Levante seeps plot at the CO<sub>2</sub>-rich range (CO<sub>2</sub>: 94.5 ± 5.9 vol%) of the global population, with only two samples having < 80% CO<sub>2</sub> (and > 20% N<sub>2</sub>).

In addition to CO<sub>2</sub>, N<sub>2</sub> and O<sub>2</sub>, hydrothermal CO<sub>2</sub> seeps contain a number of reduced gases at minor (tens of %) to trace (ppmv) levels. H<sub>2</sub>, CH<sub>4</sub> and H<sub>2</sub>S are the most commonly reported species (Table S2). Deep in the hydrothermal reservoir, these reduced trace components ultimately result from hydrothermal re-equilibration (in either vapour or liquid phase) of the feeding magmatic gas H<sub>2</sub>O, CO<sub>2</sub> and SO<sub>2</sub> at reservoir temperature, pressure and redox conditions (expressed by oxygen fugacity, fO<sub>2</sub>), according to (Giggenbach 1980, 1987):



In the reservoir, hydrothermal H<sub>2</sub>S (schematically formed by reaction (3)) can also be dissolved into the hydrothermal liquid, or precipitated into newly forming mineral phases, by a variety of reactions, among which:



where FeS<sub>2</sub>, FeS and Fe<sub>3</sub>O<sub>4</sub> are hydrothermal minerals pyrite, pyrrhotite and magnetite (native S, sulphates, and dissolved SO<sub>4</sub><sup>2-</sup>, can also be formed; Giggenbach 1980). Thus, at least to a first order, the H<sub>2</sub>, CH<sub>4</sub> and H<sub>2</sub>S contents in the hydrothermal seeps discharged at the seafloor will reflect the T–P–fO<sub>2</sub> conditions of their source reservoirs, e.g., they will record to some extent the gas compositions fixed by the T–P–fO<sub>2</sub> dependencies of relations (1) to (5), and by the extent of S scrubbing to hydrothermal brines/minerals.

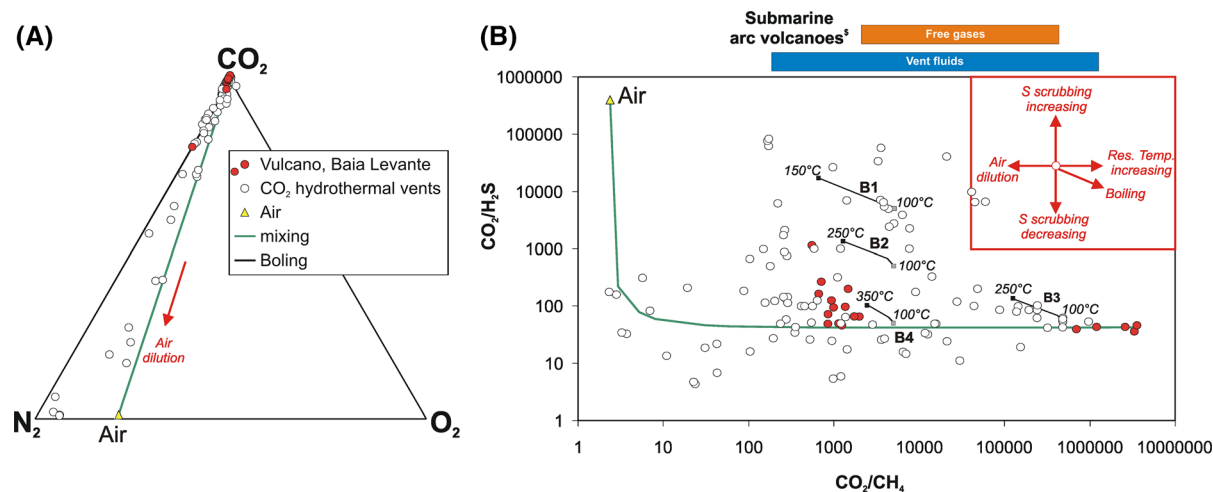


**Fig. 5** **a** Triangular plot of  $\text{CO}_2$ ,  $\text{N}_2$ , and  $\text{O}_2$  contents in hydrothermal  $\text{CO}_2$  seeps worldwide (data from Table S2). The mixing curve between pure  $\text{CO}_2$  and air is shown in green; **b** scatter plot of  $\text{CO}_2/\text{CH}_4$  vs.  $\text{CO}_2/\text{H}_2\text{S}$  ratios in hydrothermal  $\text{CO}_2$  seeps. The red arrows in the red box (top right) illustrate schematically the compositional change resulting from the different processes that govern the global variability in  $\text{CO}_2$  seep composition. Curves B1–B4 are obtained from iso-enthalpic

boiling of four distinct reservoir fluids (black squares) at 150–350 °C down to a separation temperature (grey squares) of 100 °C. Reservoir gas compositions (all in mmol/kg) are: B1:  $\text{CO}_2$ : 500,  $\text{H}_2\text{S}$ : 0.1,  $\text{CH}_4$ : 0.1; B2:  $\text{CO}_2$ : 500,  $\text{H}_2\text{S}$ : 1,  $\text{CH}_4$ : 0.1; B3:  $\text{CO}_2$ : 500,  $\text{H}_2\text{S}$ : 10,  $\text{CH}_4$ : 0.01; B4:  $\text{CO}_2$ : 500,  $\text{H}_2\text{S}$ : 10,  $\text{CH}_4$ : 0.1. These compositions are not meant to model any hydrothermal system in particular, but rather to explore the typical compositional range of hydrothermal systems in general

Because hydrothermal reservoirs can span a wide range of T–P– $f_{\text{O}_2}$  conditions (Chiodini and Marini 1998), it is not surprising that the measured  $\text{H}_2$ ,  $\text{CH}_4$  and  $\text{H}_2\text{S}$  contents in the  $\text{CO}_2$  seeps vary so widely in our catalogues, as graphically illustrated by the  $\text{CO}_2/\text{CH}_4$  vs.  $\text{CO}_2/\text{H}_2\text{S}$  scatter plot of Fig. 5b. For  $\text{CH}_4$ , part of the spread can also be justified by additional contributions from other sources/processes, including biogenic and thermogenic sources (e.g., low- and high-T organic matter decomposition) and/or abiotic methane formed by reaction other than (2) (e.g., via the Fischer Tropsch reaction) (Chen et al. 2016 and references therein). However, we cannot rule out the possibility that, for such minor components, part of the variability is due to sampling artefacts (e.g.,  $\text{O}_2$  entrainment, and consequent oxidation) and/or analytical/instrumental errors.

An additional complication is related to the contrasting aqueous solubility of  $\text{CO}_2$ ,  $\text{H}_2$ ,  $\text{CH}_4$  and  $\text{H}_2\text{S}$  at hydrothermal conditions (Giggenbach 1980), because of which these gases will differentially separate into the hydrothermal steam that forms as reservoir fluids rise (from the reservoir) toward the surface and boil (Chiodini and Marini 1998). To illustrate the effect of boiling, four distinct boiling curves (B1–B4) are shown in Fig. 5b calculated for

iso-enthalpic boiling of different hypothetical reservoir fluids (with initial  $\text{CO}_2$ ,  $\text{H}_2\text{S}$  and  $\text{CH}_4$  contents of 500, 0.1–10 and 0.001–0.1 mmol/kg). These lines are only shown for the sake of illustration, and do not attempt in any case to quantitatively mimic the trends exhibited by natural samples. Yet, the model boiling curves demonstrate that the  $\text{CO}_2/\text{CH}_4$  ratio will increase, and the  $\text{CO}_2/\text{H}_2\text{S}$  ratio will decrease, as reservoir fluids cool by iso-enthalpic boiling, from 150–350 °C (the characteristic temperature range of hydrothermal reservoirs; Chiodini and Marini, 1998) down to a separation temperature of 100° (the seafloor discharge temperature of the majority of the  $\text{CO}_2$  seeps). The curves also show that, for a given reservoir fluid composition, the ‘reservoir’ gas  $\text{CO}_2/\text{CH}_4$  ratio will increase with reservoir temperature (compares curves B1, B2 and B4 in Fig. 5b).

Because of their contrasting aqueous solubilities,  $\text{CO}_2$ ,  $\text{H}_2$ ,  $\text{CH}_4$  and  $\text{H}_2\text{S}$  can undergo additional fractionation as the rising hydrothermal steam approaches the seafloor, interacts with seawater, and eventually condenses. For example, Caracausi et al. (2005) demonstrated the chemistry of the temporal/spatial variability in the Panarea  $\text{CO}_2$  seeps in 2002–2003 was strongly linked to selective low-temperature gas dissolution in seawater during steam

condensation, perhaps in the vents' shallow feeding (conduit) systems.

The Baia di Levante CO<sub>2</sub> seeps cluster into two distinct areas (Fig. 5b). A first group is characterised by extremely high (> 100,000) CO<sub>2</sub>/CH<sub>4</sub> ratios, and have been interpreted as formed by boiling down to 100 °C of fluids ascending from a ~ 150 °C reservoir (Capaccioni et al. 2001). A second cluster of samples is characterised by lower CO<sub>2</sub>/CH<sub>4</sub> ratios (~ 1000) and somewhat higher (up to > 1000) CO<sub>2</sub>/H<sub>2</sub>S ratios, which we ascribe to a combination of (i) some extent of atmospheric dilution (many samples fall on, or nearby of, the air-pure CO<sub>2</sub> mixing line), (ii) lower reservoir temperatures (~ 100 °C; Capaccioni et al. 2001), and (iii) higher extents of S scrubbing to hydrothermal minerals (pyrrhotite, according to Capaccioni et al. 2001).

Concern has been raised (see discussion in González-Delgado and Hernández 2018) that the presence of reducing compounds (in particular H<sub>2</sub>S, being toxic for biota) in hydrothermal CO<sub>2</sub> seeps may render them unsuitable proxies for the real natural conditions of a future CO<sub>2</sub>-rich ocean. A look into the Earth's geological past shows, however, that periods characterised by high atmospheric CO<sub>2</sub> (Foster et al. 2017) have not only been associated with global ocean warming, but have also recurrently led to oceanic anoxia, where reducing gas compounds (such as H<sub>2</sub>S and CH<sub>4</sub>) do become significant (Jenkyns 2003; Meyer and Kump 2008). For example, in the high-CO<sub>2</sub> Mesozoic greenhouse world (Royer et al. 2007), a number of well-documented Oceanic Anoxic Events (OAEs) have been identified (Jenkyns 2010), such as in the early Toarcian (T-OAE; ~ 183 Ma), early Aptian (OAE 1a; ~ 120 Ma), early Albian (OAE 1b; ~ 111 Ma) and Cenomanian-Turonian (OAE 2; ~ 93 Ma). These OAEs, similarly to that at the Paleozoic–Mesozoic boundary (Wignall and Twitchett 2002), have been caused by rapid perturbation of the atmospheric carbon cycle (Hesselbo et al. 2000; Jenkyns 2010), and have led to biological crises and, in the most extreme cases, to severe mass extinctions (Wignall and Twitchett 1996; Garilli et al. 2015). If, as the geological record suggests, a link exists between swift changes in the C cycle and the establishment of reducing conditions in the ocean, it is possible that the CH<sub>4</sub>- and H<sub>2</sub>S-rich nature of hydrothermal CO<sub>2</sub> seeps may reinforce their use as proxies for ongoing/future man-made oceanic acidification.

## CO<sub>2</sub> output

The impact of shallow submarine hydrothermal CO<sub>2</sub> seeps on the chemistry of the overlying seawater column (see “[Chemical impact of hydrothermal CO<sub>2</sub> venting on the seawater column](#)” section) depends on many factors, including the geometry of the fumarolic field, the hydrodynamic properties of the seawater column itself (e.g. seawater current and any vertical stratification in temperature and density), and the CO<sub>2</sub> mass output. This latter parameter (the mass of CO<sub>2</sub> released by a hydrothermal CO<sub>2</sub> vent area/field per unit time) is critical in determining the horizontal and vertical extension of the pCO<sub>2</sub> and dissolved inorganic carbon (DIC) anomaly in seawater.

The Panarea hydrothermal field in northern Sicilian Tyrrhenian coast is the only site to our knowledge for which a systematic temporal record of the CO<sub>2</sub> output exists. Based on using a direct method, Italiano and Nuccio (1991) estimated a typical CO<sub>2</sub> output for this ~ 4 km<sup>2</sup> submarine field of ~ 9 × 10<sup>6</sup> l/day (corresponding to ~ 26–32 tons/day at the 30–100 °C temperature of the vents). This CO<sub>2</sub> output is estimated to have increased by more than one order of magnitude (up to ~ 4 × 10<sup>8</sup> l/day) in correspondence to a violent gas burst event that occurred on November 2002 (Caliro et al. 2004). Di Napoli et al. (2016) used the HydroC<sup>TM</sup>, CONTROS sensor (Fietzek et al. 2014) for real-time measurements of dissolved CO<sub>2</sub> at high temporal and spatial resolution in the seawater column above the Secca delle Fumose CO<sub>2</sub> seep field, Pozzuoli Bay (Italy). From detailed 3D mapping of pCO<sub>2</sub> in seawater, they estimated a CO<sub>2</sub> output from the Secca delle Fumose field (~ 0.14 km<sup>2</sup>) of ~ 50 tons/day (or ~ 0.53 kg/s). This is more than a factor 10 higher than the estimated CO<sub>2</sub> output from the Baia di Levante submarine seeps on Vulcano Island (~ 3.6 ton/day; Inguaggiato et al. 2012).

Hydrothermal seeps are very dynamic systems, as the deep geological processes that drive their activity can exhibit large fluctuations in time (Caliro et al. 2004). Obtaining temporal records of CO<sub>2</sub> output variations at submarine hydrothermal CO<sub>2</sub> seeps is thus a key objective of future studies.



## Aqueous fluid chemistry

In addition to gas, saline hot water (highest reported temperature, 135 °C; Price et al. 2015) is typically discharged from the seafloor by shallow hydrothermal CO<sub>2</sub> seeps (Price and Giovannelli 2017). These thermal waters can be acidic (Fig. 7) and contain bio-limiting nutrients or toxic elements (Tarasov et al. 2005; Price et al. 2013, 2015; Price and Giovannelli 2017; Pichler et al. 2019; Lu et al. 2020), so geochemical survey work was needed at Vulcano Island to map out areas well suited for ocean acidification studies, away from the influence of factors that would confound the effects of increasing CO<sub>2</sub> levels, such as toxic H<sub>2</sub>S (Boatta et al. 2013).

Hydrothermal seep fluids vary widely in composition (Figs. 6, 7) but the relative abundances of anions (Fig. 6a) and cations (Fig. 6b) is usually similar to that of seawater. Most such seeps are fed by infiltrated seawater (although there are examples of meteoric water-fed systems; Pichler et al. 1999a) with mixing with cold seawater during fluid ascent from a reservoir as well as during seafloor discharge (Price et al. 2015; Price and Giovannelli 2017). Relative to seawater, many seeps are enriched in carbon (Fig. 6a) due to CO<sub>2</sub> dissolution sourced by either hydrothermal steam (formed by steam separation from deeper reservoir fluids; Pichler et al. 1999a; cfr 3.1) or magmatic

vapours separated by the magmatic source (Caliro et al. 2004). Sulfur is typically depleted relative to seawater due to deposition of hydrothermal sulphates (Alt 1995; German and Von Damm 2003) and sulphides (Hannington et al. 2011) upon hydrothermal infiltration and maturation (Fig. 6a).

One notable feature of vent fluids (or, at least, of those poorly affected by near-surface mixing with seawater) is their characteristic Mg depletion (Figs. 6b, 7a), which arises from extensive Mg removal from solutions due to formation of hydrothermal phyllosilicates (German and Von Damm 2003; Tivey 2007). Prior to mixing with seawater, hydrothermal vent fluids are, in the majority of the cases, of alkali-chloride composition (Fig. 6b), as typical of ‘mature’ geothermal waters that have attained full-equilibrium conditions after prolonged fluid-rock interaction with the host rocks at hydrothermal reservoir P–T-conditions (Giggenbach 1988). These fluids exhibit a range of alkalis/Ca ratios (Fig. 6b), reflecting different extents and environments (P–T-conditions) of fluid–mineral interaction from one seep system to another, or even within one single system (Price et al. 2015; Price and Giovannelli 2017).

Vent fluids exhibit a wide range of salt contents, as exemplified for Na in Fig. 7b, implying a multiplicity of sources and processes. A large cluster of seeps plot at Na concentrations slightly lower than seawater, suggesting seawater recharge followed by some extent of Na removal by hydrothermal minerals (e.g., albitization; Tivey 2007) during mineral–fluid interaction. The numerous vents with Na contents plotting well above (e.g., a subset of vents samples from Milos and Panarea) or below (e.g., Tatum bay) seawater (Fig. 7b), point to additional processes, however, and indicate in particular the recurrence of phase separation processes (Butterfield et al. 1990; Von Damm et al. 2003; Foustoukos and Seyfried 2007). Supercritical (above critical point) phase separation (Hedenquist and Lowenstern 1994) deep in the Panarea hydrothermal system has for example being invoked (Price et al. 2015) to explain the formation of saline brines (Na > 600 mM) vented by some seeps (Fig. 7b); while low salinity vent fluids (Na < 400 mM) have recurrently been explained (Pichler et al. 1999a; Price et al. 2013, 2015) by near-surface condensation of hydrothermal steam, formed by sub-critical phase separation (boiling) at depth.

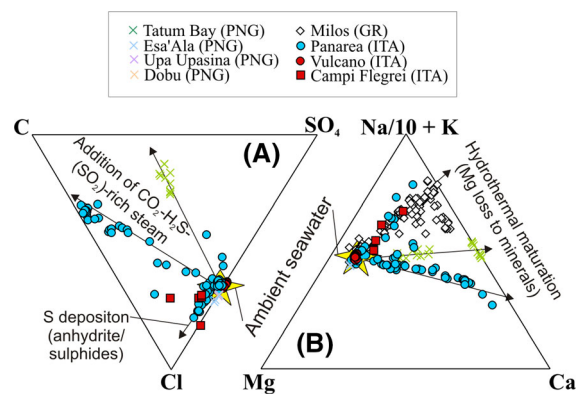


**Fig. 6** Triangular plots for anion (a) and cation (b) contents in some selected, well-studied seeps. Data used to draw the plots are listed in Supplementary Table S3. *Data Sources* Milos: Valsami-Jones et al. (2005), Price et al. (2013), Lu et al. (2020); Tatum bay, PNG: Pichler et al. (1999a), Pichler et al. (2019); Vulcano Island: Sedwick and Stuben (1996), Boatta et al. (2013); Panarea: Italiano and Nuccio (1991), Caracausi et al. (2005), Price et al. (2015); Upa-upasina, Dobu, Esa'Ala, PNG, Fabricius et al. (2011); Campi Flegrei: Di Napoli et al. (2016)

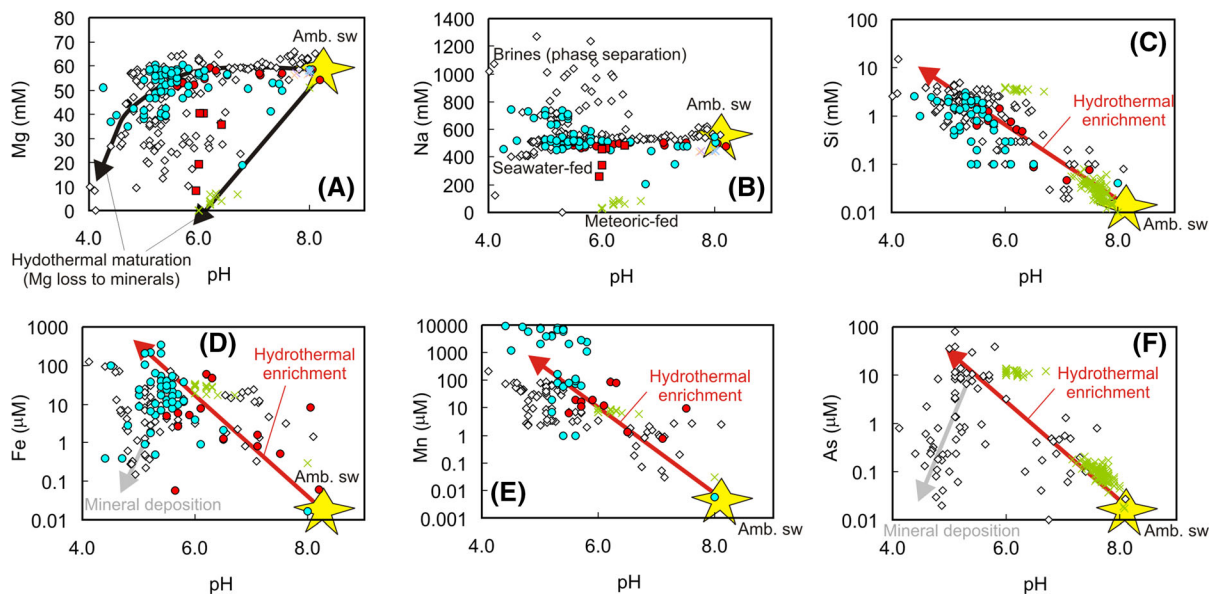


**Fig. 7** Scatter plots of pH vs. selected major (Mg, Na), minor (Si) and trace (Fe, Mn, As) contents in some selected seeps (and in the overlying seawater column). Symbols and data-sources are as in Fig. 6

Prolonged high-temperature interactions with reservoir rocks enrich hydrothermal fluids in a suite of minor elements such as Si (Fig. 7c), alkalis (Li, Rb, Cs) and B (Giggenbach 1997). Some of these elements (e.g., Si, B) exhibit conservative behaviour (e.g., they remain in dissolved forms during mixing of seep waters with seawater, and cooling; Fig. 7c), and can thus serve to quantify the extent of seawater entrainment (the mixing proportions of hydrothermal and marine components in the seeps; Italiano and Nuccio 1991; Pichler et al. 1999a, 2019; Caracausi et al. 2005), and to map dispersion and dilution of seep-derived elements into the seawater column (Pichler et al. 1999a, 2019).

The hot, reducing conditions of hydrothermal systems mobilise trace elements (e.g., Fe, Mn, Cu, Pb, Zn, Cd, As, and many others) by leaching from rocks, leading to orders of magnitude enrichment in seeps relative to seawater (see Tarasov et al. 2005) (Fig. 7d–f). Trace elements play a wide range of possible roles in (and effects on) living organisms, from essential/bio-limiting to harmful/toxic (Stumm and Morgan 1995; Rainbow 2002). As such, care is needed when using these systems as natural proxies or studying OA effects on marine organisms. Trace element contents in seawater surrounding hydrothermal seeps have been measured in several cases,

including at Vulcano Island, the main focus of this paper (Boatta et al. 2013; Brinkman 2014; Donnarumma et al. 2019; Pichler et al. 2019; Zitoun et al. 2020). Bio-availability of trace-elements depends on metal speciation (Rainbow 2002; Vizzini et al. 2013; Mishra et al. 2020) and so seeps provide areas in which to assess the effects of ocean acidification on trace element toxicity. One key aspect to address is to assess which metals precipitate to minerals upon contact with cold seawater (e.g., Pichler et al. 1999b; Becke et al. 2009; Price and Pichler 2005; Price et al. 2013) and which dissolve and disperse to potentially have wider-scale consequences on ecosystems.

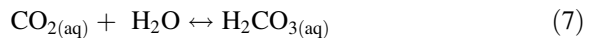
The trace-element vs. pH trends illustrated in Fig. 7d–f offer some useful (though preliminary) clues. The Mn vs. pH plot of Fig. 7e, for example, shows a relatively uniform trend of increasing Mn concentrations (of up to 7 orders of magnitude above seawater) at increasingly acidic (pHs of 4–7) seep conditions. This points to relatively wide Mn mobility over a range of aqueous environments (Lupton et al. 2011). In contrast, Fe (Fig. 7d) and As (Fig. 7f) show more complex behaviours when plotted vs. pH. Although we cannot rule out these trends partially reflect unsuccessful sampling of pure hydrothermal end-members, we consider more likely that the observed contrast between Mn and Fe/As behaviours

imply non-conservative behaviour and scavenging of the latter elements to mineral phases (e.g., oxy-hydroxides and sulphides; e.g., Pichler and Veizer 1999; Pichler et al. 1999a, b; Becke et al. 2009; Price and Pichler 2005; Price et al. 2013) upon mixing/cooling in the upflow zone (especially at  $\text{pH} < 5.5$  and 7; Fig. 7). Extensive work on As, in particular, has shown that while this element can be extremely enriched in seeps (Pichler et al. 1999a, b; Price et al. 2013), only moderate enrichments in the overlying seawater column (relative to reference seawater) are produced owing to extensive precipitation of As-rich oxy-hydroxides upon seep discharge (Pichler and Veizer 1999). This fact, combined with lack of visible impacts on coral communities, led Pichler et al. (2019) to conclude that the high As load transported by those seeps did not result in major biological consequences. This topic has been examined in most detail with regard to seagrasses, since the question arose as to why they thrive at some  $\text{CO}_2$  seeps but not others. At some seeps seagrasses are abundant where  $\text{CO}_2$  bubbles up through the seabed, and the plants are thought to benefit from the increased availability of Dissolved Inorganic Carbon for photosynthesis and a decreased cover of epiphytic coralline algae on their leaves (Martin et al. 2008; Russell et al. 2013). However seagrasses do badly close to some  $\text{CO}_2$  seeps due to  $\text{H}_2\text{S}$  and/or metal toxicity (Vizzini et al. 2013). At Vulcano and other Mediterranean seeps areas with bioavailable toxins can be avoided by moving away from the seeps to where levels of seawater  $\text{CO}_2$  are below  $1000 \mu\text{atm}$  (Mishra et al. 2020), although bioavailable species can occasionally reach toxic thresholds in these more distal environments, too. The conclusion is that, although geochemical surveys of seep sites are warranted, trace element enrichment in shallow hydrothermal  $\text{CO}_2$  vents should not prejudice their use as natural proxies for OA studies. However, as seeps are very dynamic multiple stressor environments, areas suitable for OA studies must be carefully selected using comprehensive (gaseous, major, minor and trace aqueous species) chemical characterization.

## Chemical impact of hydrothermal $\text{CO}_2$ venting on the seawater column

$\text{pCO}_2$  distribution in seawater

Upon exiting the seafloor,  $\text{CO}_2$  bubbles vented from the seeps dissolve into seawater (Fig. 1), via reactions:



$\text{CO}_2$  can dissolve either partially or totally in the seawater column, depending on seep discharge rate ( $\text{CO}_2$  output; cfr. 3.2) and vent emission depth. If the  $\text{CO}_2$  output is high enough, and the seawater column only shallow, part of the gas can freely escape at the seawater–air interface, leading to gas bubbling at surface (Fig. 1). In both cases, the ultimate effect is to raise seawater Total Dissolved Inorganic Carbon (TDIC) and  $\text{CO}_2$  partial pressure ( $\text{pCO}_2$ ).

Traditionally, seawater  $\text{pCO}_2$  values in the surroundings of hydrothermal  $\text{CO}_2$  seeps have been determined by numerically solving dissolved C speciation from co-measured TDIC and pH. Results obtained at the different  $\text{CO}_2$  seeps worldwide, illustrated in Fig. 8a, demonstrate a transition from ‘normal seawater’  $\text{pCO}_2$  ( $\sim 400 \mu\text{atm}$ ) in background (control) sites far from the vents, to circa  $\sim 1000 \mu\text{atm}$  at “intermediate” (meters to tens on meters) distance from the vents, to exceptionally high  $\text{pCO}_2$ s ( $\geq 10,000 \mu\text{atm}$ ) in near-vent conditions. The most extreme  $\text{pCO}_2$  conditions (up to  $52,000 \mu\text{atm}$ ) have been observed offshore Ischia volcano, in Italy (Hall-Spencer et al. 2008). It is along  $\text{pCO}_2$  gradients of  $300\text{--}1000 \mu\text{atm}$  that biological research focuses in the attempt to characterise the response of biological communities to enhanced seawater  $\text{CO}_2$  levels (Agostini et al. 2018; see “Biological experiments at volcanic  $\text{CO}_2$  seeps as analogues of ocean acidification” section).

The advent of novel, portable instruments for real-time measurement of dissolved  $\text{CO}_2$  in seawater is now paving the way to mapping seawater  $\text{pCO}_2$  distribution around hydrothermal seeps at much finer spatial resolution (e.g., Di Napoli et al. 2016). In our Baia di Levante example, we used a HydroC<sup>TM</sup>  $\text{pCO}_2$  sensor (from CONTROS Systems and Solutions, Fietzek et al. 2014) and a multi-parameter probe (Ocean Seven 303 CTD, IDRONAUT) to map the

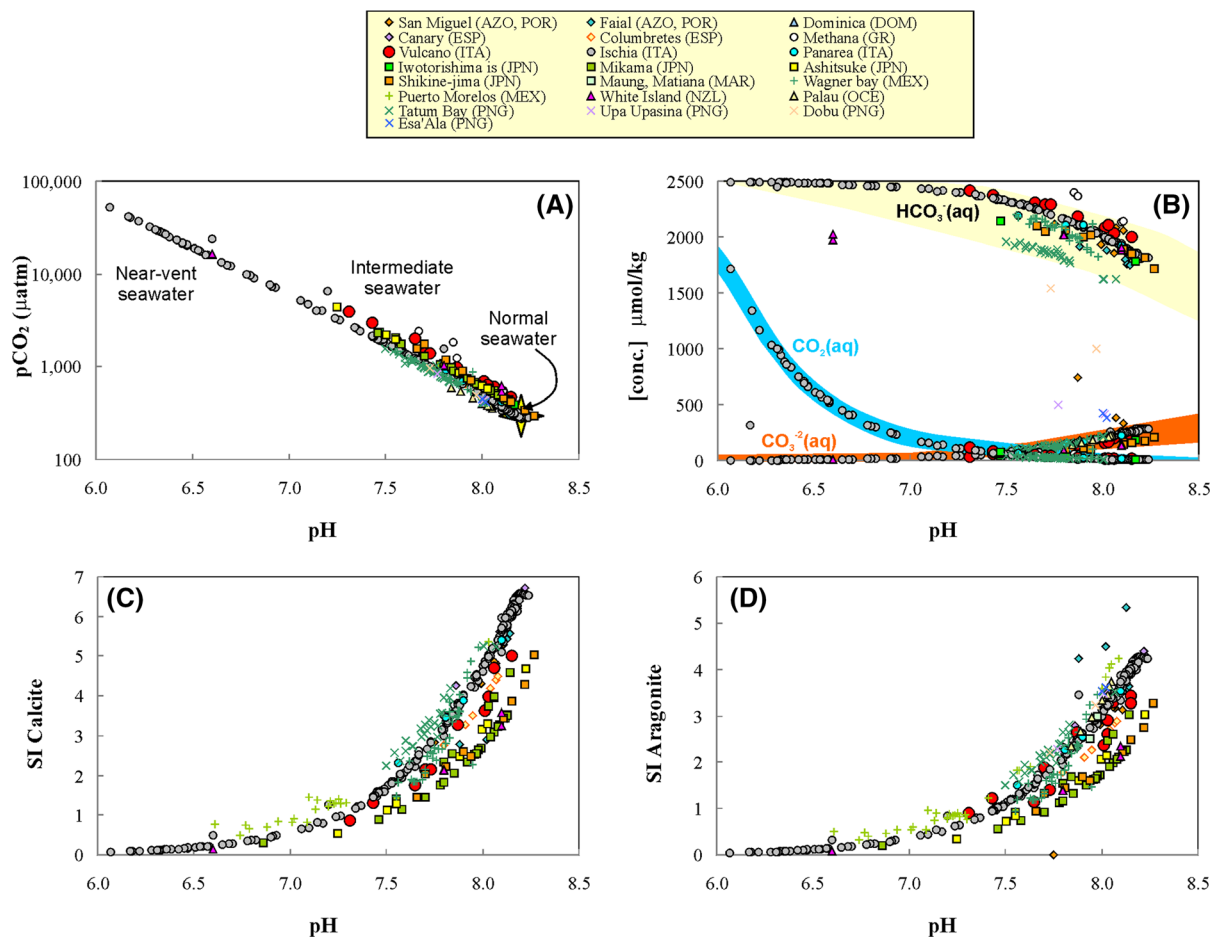


**Fig. 8** Scatter plots illustrating seawater carbon chemistry at hydrothermal  $\text{CO}_2$  seeps worldwide (data from Table S4). **a** pH vs.  $\text{pCO}_2$ ; **b** pH vs. dissolved C species; **c** pH vs. calcite Saturation Index (SI); **d** pH vs. aragonite Saturation Index (SI).

$\text{pCO}_2$  in the bay (Fig. 9a, b). The  $\text{pCO}_2$ s obtained from both sensors (HydroC<sup>TM</sup> and Ocean Seven 303) matched well those derived from traditional techniques (Capasso and Inguaggiato 1998) that use directly sampled seawater samples (see Fig. 9c), providing further validation for these new generations of instruments (Fietzek et al. 2014).

Here, we used a small boat to profile the bay along the track shown in Fig. 4, while our sensor kit was continuously acquiring data (at 1 Hz rate). From this, the lateral variability of seawater  $\text{pCO}_2$  at a constant depth ( $\sim 0.5$  m) was obtained, which is ultimately illustrated by the map of Fig. 9. The map demonstrates the ability of these novel sensor kits to finely resolve (in real-time) dissolved  $\text{CO}_2$  in seawater around seeps

$\text{pCO}_2$ , dissolved C speciation and SIs are equilibrium values calculated from measured pH and Total Dissolved Inorganic Carbon (TDIC)

with much improved spatial resolution than possible with traditional methods (direct sampling). We recommend increased use of these sensors in future OA and seabed carbon capture and storage studies.

#### pH and ocean acidification

The dissolution of  $\text{CO}_2$  in seawater around seeps has several environmental consequences. The dissociation of the carbonic acid ( $\text{H}_2\text{CO}_{3(\text{aq})}$ ; see relation (7)) lowers the pH (Fig. 8a), alters the normal seawater dissolved carbon speciation (Fig. 8b), and lowers the seawater saturation state of calcite and aragonite (Fig. 8c, d). At intermediate conditions, meters to tens of meters from the seeps, seawater acidity is typically

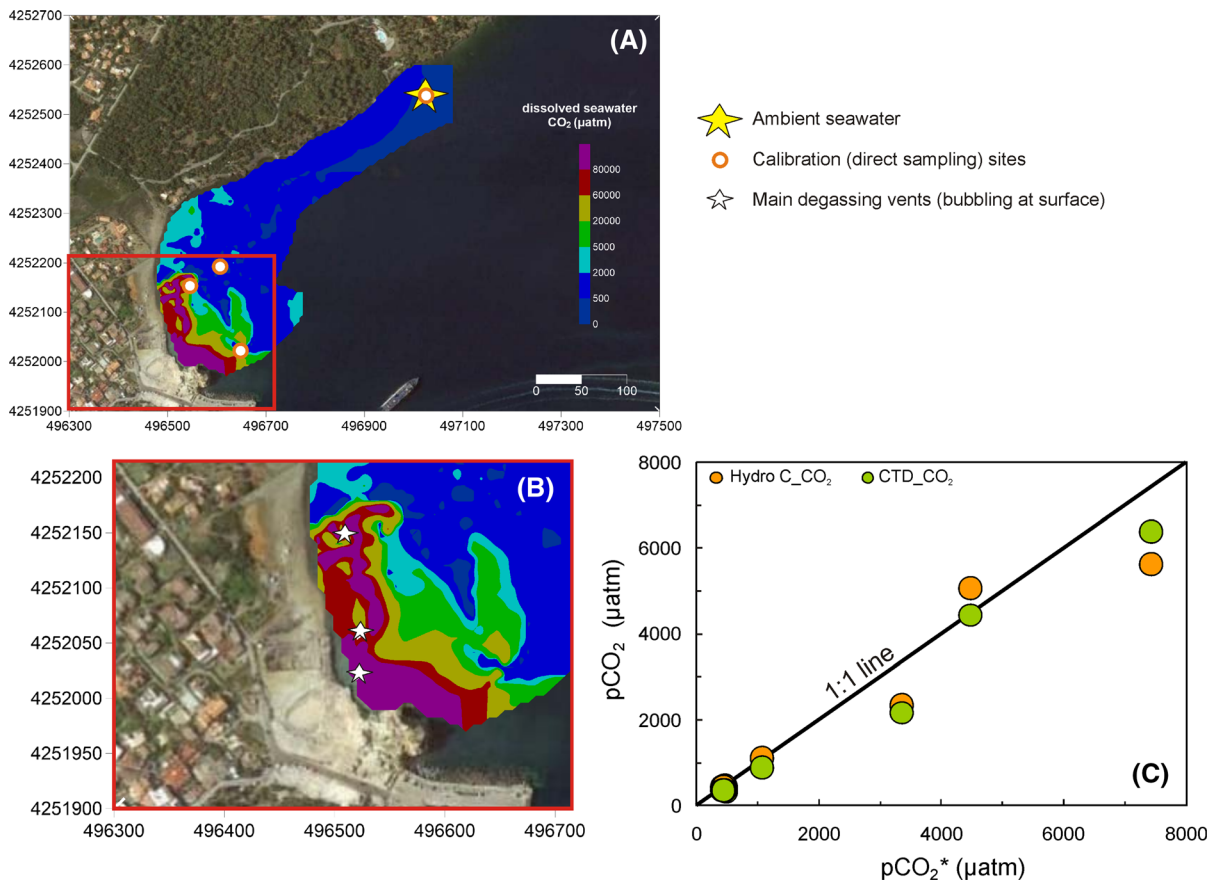


**Fig. 9** **a** A map of seawater pCO<sub>2</sub> distribution in the Baia di Levante bay. The map was generated from in-situ real-time measurements of dissolved CO<sub>2</sub>, obtained using a HydroC<sup>TM</sup> sensor (for CO<sub>2</sub> < 6000 μatm) and an Ocean Seven 303 IDRONAUT CTD (for CO<sub>2</sub> > 6000 μatm). Measurements were obtained using a small boat and profiling along the track shown in Fig. 4 (bottom, right). The use of the HydroC<sup>TM</sup> and IDRONAUT CTD sensors to measurement of dissolved CO<sub>2</sub> in seawater was initially validated against results from conventional direct sampling, as shown in (c). Water samples for sensor comparison were collected in sites indicated by white circles; **b** a detail of (a). Stars identify the position of the main degassing vents (where gas bubbling at the free seawater surface was also concentrated); **c** comparison between pCO<sub>2</sub> values measured by

the HydroC<sup>TM</sup> sensor (orange diamonds) and the Ocean Seven 303 IDRONAUT CTD (green diamonds) (both on the y-axis) and those measured with the direct sampling technique of Capasso and Inguaggiato (1998) method (x-axis). The dashed line represents the 1:1 line (e.g., it identifies perfect match between instrumental and direct sampling derived pCO<sub>2</sub>s). The best-fit regression lines are respectively:  $y = 0.99x - 65$ ,  $R^2 = 0.93$  (for direct vs. HydroC<sup>TM</sup> datasets) and  $y = 0.87x - 27$ ,  $R^2 = 0.99$  (for direct vs. IDRONAUT CTD datasets). Overall, our test shows that the HydroC sensor pCO<sub>2</sub> results are well consistent with those derived in laboratory on the directly sampled seawater samples (method of Capasso and Inguaggiato 1998). This agreement provides mutual validation for the 3 techniques. (Color figure online)

up to 0.2–1 log units lower (pH of 8 to 7) than ambient seawater (Fig. 8a), dissolved CO<sub>2(aq)</sub> concentrations increases at the expense of the carbonate ion (CO<sub>3</sub><sup>2-</sup><sub>(aq)</sub>) (the two species attain similar abundances at pH ~ 7.5, while CO<sub>2(aq)</sub> prevails over CO<sub>3</sub><sup>2-</sup><sub>(aq)</sub> at pH < 7.5; Fig. 8b), and the calcite/aragonites Saturation Indexes (SIs) drop, from ~ 4–6 to ~ 1–2 (Fig. 8b, c). In the most extreme conditions (in the near-vent environment), where pCO<sub>2</sub> exceeds 10,000

μatm, the pH becomes acidic (6.5 to 6; Fig. 8a) and CO<sub>3</sub><sup>2-</sup><sub>(aq)</sub> concentrations are largely suppressed (Fig. 8b), ultimately unstabilising carbonate minerals (Fig. 8c, d). The same transition, from 'normal seawater' to 'acidified seawater' conditions can be captured by independent pCO<sub>2</sub> and pH measurements while approaching the active seeps, as in our Baia di Levante example (Fig. 10).

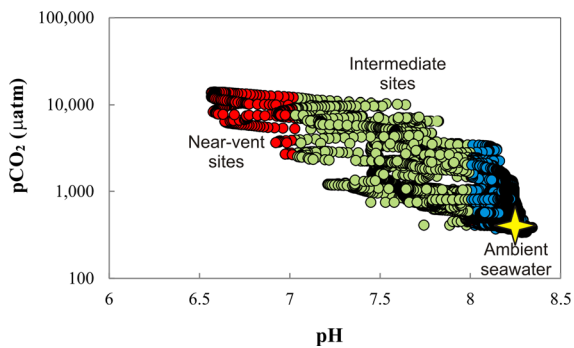


**Fig. 10** Seawater pH vs.  $p\text{CO}_2$  scatter plot at Baia di Levante (Vulcano Island). pH was measured with the Ocean Seven 303 IDRONAUT CTD, while  $p\text{CO}_2$  was real-time in-situ determined via either the HydroC<sup>TM</sup> sensor (for  $p\text{CO}_2 < 6000 \mu\text{atm}$ ) or the Ocean Seven 303 IDRONAUT CTD (for  $p\text{CO}_2 > 6000 \mu\text{atm}$ ). Measurements were taken at constant seawater depth at a constant depth of  $\sim 0.5$  m along the measurement grid shown in Fig. 4. We categorize samples in near-vent sites ( $\text{pH} < 7$ ), intermediate sites ( $7 < \text{pH} < 8$ ) and near-ambient sites ( $\text{pH} > 8$ ). These three categories correspond to distances from the vent areas of  $< 10$  m,  $10\text{--}100$  m and  $> 100$  m, respectively

#### Biological experiments at volcanic $\text{CO}_2$ seeps as analogues of ocean acidification

In addition to their global significance in geological  $\text{CO}_2$  flux, many submarine seeps provide opportunities to improve predictions about the effects of OA on the marine biota and ecosystem structure and function. Such seeps allow assessments of the effects of high  $\text{CO}_2$  levels and lowered seawater pH on spatial and temporal scales sufficiently large to set up experiments to address responses from individual organisms to ecosystems (Gaylord et al. 2015; Hall-Spencer and Harvey 2019). Most research using seep sites to assess the biological effects of OA have avoided localised areas with raised temperature, anoxia and/or toxic metals (Boatta et al. 2013) (Fig. 9), although such sites provide ample opportunities to assess the combined effects of multiple stressors. In this regard, a recent attempt was made along the  $p\text{CO}_2/\text{pH}$  gradient off Vulcano Island (Southern Italy), combining the naturally occurring carbonate chemistry gradient with an in-situ manipulation of temperature conditions and assessing how these environmental stressors affect the fitness of a reef building species. Under an end of the century scenario of both stress factors ( $\sim 1000 \mu\text{atm}$  and  $+ 2^\circ\text{C}$ ) transplanted vermetid reefs exhibited compromised oxygen consumption and bio-

mineralization processes leading to impaired development and recruitment (Alessi et al. 2019).

Two types of experiments are generally employed to investigate the effects of OA at  $\text{CO}_2$  seeps: observational and transplantation experiments. In-situ observational experiments assess the species responses along natural pH gradients, generally moving progressively away from the most intense  $\text{CO}_2$  bubbling site to ambient  $\text{CO}_2$  sites both in intertidal and subtidal zones (e.g. Agostini et al. 2018). Such experiments usually focus on sessile benthic species which are chronically exposed to the  $p\text{CO}_2$  and pH gradient moving away from the seep site (Agostini et al. 2018). This approach has also highlighted mechanisms underpinning evolutionary responses of calcifying species in past OA events (Garilli et al. 2015).

In-situ observational studies often precede experiments involving field transplantations where researchers, in the attempt to highlight cause-effect mechanisms, compare responses of single species or entire assemblages and communities to both short- and long-term acidified and natural control conditions (Camp et al. 2018). For practical reasons, most experiments at  $\text{CO}_2$  seeps have focused on low motility benthic stages of organisms, such as microbes, macroalgae, anemones, corals, sessile polychaetes, bryozoans, or bivalve and gastropod molluscs (e.g. Goffredo et al. 2014) rather than planktonic, neustonic or highly mobile organisms such as phytoplankton, cephalopods or fish.

Biological studies at  $\text{CO}_2$  seeps include the experimental investigation of processes such as calcification/dissolution, growth, survival, settlement, recruitment, reproduction, metabolic performance, behaviour, species interactions and community shifts in relation to spatio-temporal changes in pH,  $p\text{CO}_2$  and saturation levels of aragonite and calcite (Camp et al. 2018). In some instances,  $\text{CO}_2$  seep research has provided evidence of direct physiological impacts on individuals living along  $\text{CO}_2$  gradients, causing impaired growth and reproduction, and hence affecting the population level under elevated  $p\text{CO}_2$  conditions (Harvey et al. 2016). Other experiments document shifts in habitat-forming species and consequent reshuffling of species at community-level or imbalanced function at ecosystem-level (e.g., Vizzini et al. 2017; Milazzo et al. 2019). Despite the obvious caution needed to avoid confounding factors,

biological experiments carried out at CO<sub>2</sub> seeps currently provide a powerful tool to assess future ocean conditions, especially for documenting which organisms and processes are most resilient to OA and to assess potential risks for marine populations, communities and ecosystems.

#### Winners and losers at natural analogues of OA: the Baia di Levante case study

How organisms will respond to OA might depend on energetic trade-offs between the physiological costs of maintaining ion regulation and acid base status and other energetically demanding processes, such as growth, calcification, reproduction, and activity. These determine the life-history traits and therefore the performance and fitness of the organisms. Such responses may be limited not only by a species' physiological plasticity but also by energy availability in the environment. Despite recent advances in understanding the energetic trade-offs that determine species sensitivity to OA in the laboratory, CO<sub>2</sub> seep studies are only starting to reveal how these trade-offs can be affected under natural conditions where species are subjected to additional biotic and abiotic processes that can modify interactions and energy availability (Garilli et al. 2015; Turner et al. 2015).

Meta-analyses of laboratory responses to OA shows that sensitivity varies among life stages, species and broader taxonomic groups (Hendriks et al. 2010; Kroeker et al. 2010, 2013; Harvey et al. 2013; Wittmann and Pörtner 2013; Cattano et al., 2018), although it is difficult to know how this range of responses plays out in the real world without empirical data from natural gradients in OA conditions (Rastrick et al. 2018). Here, we consider the culmination of complex responses of organisms to OA by assessing changes in the abundances of organisms in-situ using effect size analysis (Hedges et al. 1999) along gradients of OA off Vulcano Island (Aeolian Islands, Sicily) (Fig. 11), one of the most intensively used natural laboratories for OA research.

To make comparisons at different pCO<sub>2</sub> levels along the gradient we considered a CO<sub>2</sub> range ( $\Delta$ CO<sub>2</sub>) as the difference between the CO<sub>2</sub> concentration in elevated, intermediate, near-ambient and the control CO<sub>2</sub> condition, that resulted as extreme ( $\Delta$ CO<sub>2</sub>  $\geq$  750  $\mu$ atm), intermediate (750 >  $\Delta$ CO<sub>2</sub> > 350  $\mu$ atm) and

moderate ( $\Delta$ CO<sub>2</sub>  $\leq$  350  $\mu$ atm) OA scenarios (Fig. 11).

Our analyses suggest that primary producers like benthic biofilm (cyanobacteria and diatoms), filamentous turf and fleshy algae showed similar magnitude of mean increases in abundance in OA conditions (Fig. 11), as found by Harvey et al. (2019) at Japanese CO<sub>2</sub> seeps. The abundance of crustose coralline algae was not affected under OA, and bivalve abundances increased in extreme low pH/high CO<sub>2</sub> conditions, which are surprising results given that coralline algae and bivalves have been shown to be adversely affected by OA at volcanic seeps in Papua New Guinea and Japan (Fabricius et al. 2015; Agostini et al. 2018) and the Azores (Martins et al. 2020). However, the proliferation of a few hardy taxa and the demise of many others is a common feature in OA research and a reduction in diversity (rather than abundance) can impair ecosystem services (Hall-Spencer and Harvey 2019). Other calcified taxa showed consistent reductions in abundance in the extreme OA scenario, which were similar among coccolithophores, gastropods, bryozoans and serpulid worms. Our evidence that marine taxa potentially vulnerable to low pH conditions may in some instances thrive under OA is not new, as local environmental conditions like nutrient availability (Connell et al. 2017) or exposure over multiple generations (Cornwall et al. 2020), may help some organisms to thrive (Zitoun et al. 2020).

Consistent increases in abundance in OA conditions were detected for anemones, isopods, amphipods, and other polychaetes at all lower pH/elevated pCO<sub>2</sub> levels considered. No effects of acidification were detected on fish abundances (Fig. 11). Our analyses reveal that the magnitude of responses to OA in the field varies among examined groups, suggesting variation in sensitivity when multi-species assemblages are considered with this having important implications for ecosystem responses under OA conditions.

If we look at species diversity, most algal species are resilient to OA, with only around a 5% loss in species diversity at levels projected under the IPCC RCP 8.5 (Brodie et al. 2014). Increased carbon availability stimulates primary production. This can increase the standing stock of kelps and seagrasses (Russell et al. 2013; Linares et al. 2015; Cornwall et al. 2017) although microalgal biofilm and weedy small turf algae dominate at high CO<sub>2</sub> levels in exposed

### Effect sizes on abundances of key taxonomic groups at Vulcano Island

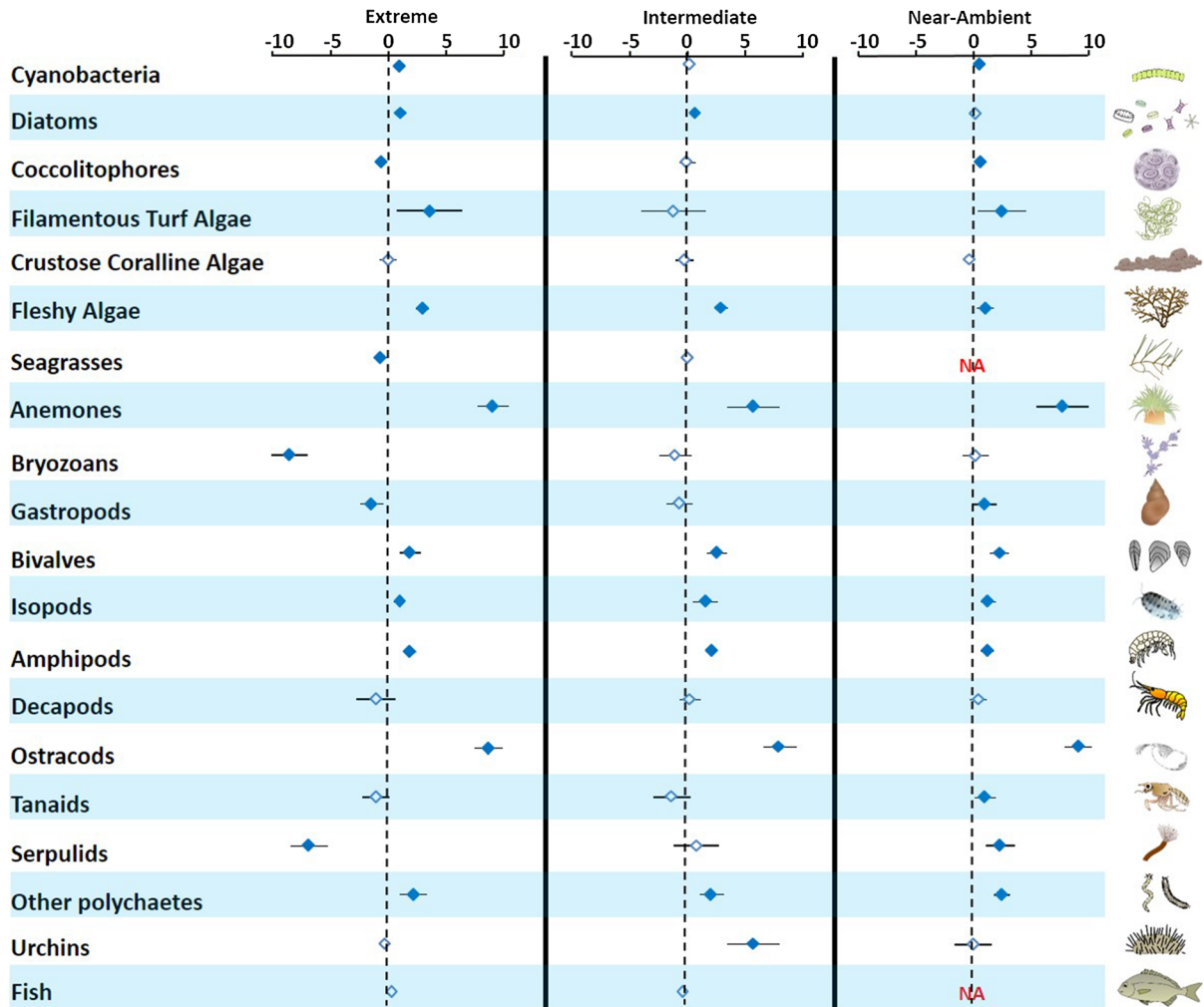


**Fig. 11** Effect sizes ( $\pm$  95% CI) on abundances of different key taxa at Baia di Levante (Vulcano Island, Italy). For each response variable, the response ratio (RR) was calculated with Extreme, Intermediate and near Ambient  $\text{CO}_2$  conditions as numerators (i.e., the experimental condition) and the Control condition as the denominator. Empty diamonds represent null effects, while filled ones represent positive or negative significant effects. The response of each group to different pH conditions was analysed using %cover for Cyanobacteria, Diatoms, Coccolithophores, Filamentous turf algae, Crustose coralline algae, Fleshy algae, shoot density for Seagrasses, and

density for Anemones, Bryozoans, Gastropods, Bivalves, Isopods, Amphipods, Decapods, Ostracods, Tanaids, Serpulids, other Polychaetes, Sea Urchins and Fish (as MaxN relative abundance). Data from: Suggett et al. (2012), Calosi et al. (2013), Johnson et al. (2013), Ziveri et al. (2014), Apostolaki et al. (2014), Nagelkerken et al. (2015), Harvey et al. (2016); Vizzini et al. (2017), Milazzo et al. (2019), Mishra et al. (2020); Turco G. unpublished data. Images from <https://notendur.hi.is/~salvor/myndvinnsla/inkscape/IAN%20symbol%20Libraries%205.1%20SVG/>

conditions (Agostini et al. 2018; Connell et al. 2018). Shifts in algal community composition greatly alter habitat characteristics (Brodie et al. 2014; Enochs et al. 2015) with this having major implications on associated invertebrate and vertebrate fauna (Fabricius et al. 2014; Cattano et al. 2020).

At tropical, sub-tropical and temperate seeps there is a shift to less diverse coastal ecosystems as  $\text{pCO}_2$  levels increase. There is around a 30% fall in animal biodiversity as average pH declines from 8.1 to 7.8 (Fabricius et al. 2011; Agostini et al. 2018; Foo et al. 2018). This is due to direct and indirect effects, such



increased metabolic costs of coping with hypercapnia or increased susceptibility to predation (Sunday et al. 2017). A diverse range of invertebrates build reefs; such as sponges, corals, serpulids, vermetids, oysters, mussels and bryozoans. Reefs are degraded along gradients of decreasing carbonate saturation, due to increased metabolic costs of calcification, chemical dissolution and enhanced bioerosion.

Opportunistic organisms can more easily adapt to acidification (Kroeker et al. 2011; Brown et al. 2018). In the tropics, some corals are able to grow well in acidified conditions, but the habitats they form lack complexity and the reef itself is eroded (Fabricius et al. 2011). These degraded reefs have more fleshy macroalgae, less calcified algae and tend to have fewer invertebrates. The dual effects of increased CO<sub>2</sub> and decreased carbonate alter trophic interactions in both sub-tropical and temperate coastal systems. Reductions in the abundance and size of calcareous herbivores contribute to the overgrowth of weedy turf algae and a simplification of food webs, with losses in functional diversity (Vizzini et al. 2017; Teixidó et al. 2018). In this regard, marine ecosystem services depend on what basic biotic functions are maintained (Connell et al. 2018), which ecosystem engineers and keystone species are retained (Sunday et al. 2017), and whether the spread of nuisance species is avoided (Hall-Spencer and Allen 2015).

#### Ecosystem effects of OA at CO<sub>2</sub> seeps

In the past 10 years, experimental work using natural gradients in pCO<sub>2</sub>/pH has increased worldwide. The ecosystem effects of acidification were first described on a range of coastal Mediterranean habitats off the Castello Aragonese in Ischia Island (Italy). In this shallow seep site, CO<sub>2</sub> bubbling up through the seabed gradually lowers the pH of the water column from present day ambient pH 8.2, through near future pH 7.9, down to worse case predictions of pH 7.4 in the immediate vicinity of seeps (Hall-Spencer et al. 2008). Along these pCO<sub>2</sub> and pH gradients, rocky shore communities with abundant calcareous organisms shift to communities lacking sea urchins, scleractinian corals and vermetid molluscs and with significant reductions in coralline algae. This approach has provided an ecosystem-scale validation of laboratory-based predictions that important groups of

organisms are susceptible to elevated levels of pCO<sub>2</sub> in the ocean.

Since then, evidence from CO<sub>2</sub> seeps including coral (Fabricius et al. 2011, 2014; Inoue et al. 2013; Enochs et al. 2015; Agostini et al. 2018) and other calcifying reefs (Milazzo et al. 2014; Linares et al. 2015; Alessi et al. 2019), seagrasses (Garrard et al. 2014; Nagelkerken et al. 2015), and algal dominated habitats in temperate zones (Porzio et al. 2011) has notably increased, showing community structure alterations in response to OA (Fig. 12).

A reduction in community complexity is expected following prolonged exposure to OA (e.g. Kroeker et al. 2011; Sunday et al. 2017), primarily due to the loss of CO<sub>2</sub>-sensitive species (e.g. calcifying habitat-forming species) and an increase in primary producers (e.g. fleshy algae and turf-forming algae) boosted by elevated CO<sub>2</sub> conditions (Connell et al. 2018). This shows the dual role of CO<sub>2</sub> as a stressor and a resource for marine ecosystems. Biotic homogenization occurs under OA, with systems at low disturbance (i.e. ambient CO<sub>2</sub> and pH) hosting specialist species with high complementarity and high ecosystem function, while highly disturbed ecosystems (elevated CO<sub>2</sub> and low pH) favoring generalist species and homogenized communities with low function.

Vermetid reef communities transplanted for one year along CO<sub>2</sub> gradients off Vulcano Island, revealed dominance shifts from reef- to non reef-forming habitats (Milazzo et al. 2019). These shifts led to changes in composition, structure and functional diversity of the associated benthic assemblages. Interestingly, community properties (i.e. species richness and abundance) nonlinearly responded to OA conditions, high-order consumers (e.g. carnivores) failed to compensate, and competitive release of minor herbivores occurred under elevated CO<sub>2</sub> levels (Milazzo et al. 2019). Coastal community assemblages often have low functional redundancy (Micheli and Halpern 2005), meaning that CO<sub>2</sub>-tolerant species performing a similar functional role may not exist. This suggests the likelihood for the loss of functional traits and groups (e.g. reef-forming species and carnivores) (Sunday et al. 2017; Vizzini et al. 2017; Teixidó et al. 2018), while highlighting the potential for opportunistic species to become more generalist and widen their ecological niche.

Shallow biogenic reefs are particularly sensitive to OA, the degradation of these habitats results in less



**Fig. 12** Evidence of community shifts from ambient to elevated  $\text{CO}_2$  levels off a seep site in Papua New Guinea. In ambient locations highly complex and diversified coral reef species

which shift into low profile corals and fleshy algae in elevated  $\text{CO}_2$  conditions close to the bubbling site. Photo credit: Marco Milazzo

coastal protection and less habitat provisioning for biodiversity and fisheries. Live coral cover on tropical reefs has nearly halved in the past 150 years, and the decline dramatically has accelerated over the past 2–3 decades due to increased water temperature and OA interacting with and further exacerbating other drivers of loss. Natural gradients in seawater  $\text{CO}_2$  show that risks to marine goods and services amplify with increasing carbon emissions. When combined with rising temperatures, sea level rise and increasing extreme events, OA further threatens the goods and services provided by coastal ecosystems. This is particularly important for those people and countries that are heavily reliant on marine resources for protection, nutrition, employment and tourism (Lam et al. 2019).

## Summary

We have reviewed existing knowledge on the geochemistry and ecology of submarine volcanic  $\text{CO}_2$  seeps, especially focusing on the lessons these studies bring for predicting the potential impact of OA under a growing atmospheric  $\text{CO}_2$  planet. We have shown that volcanic seeps are  $\text{CO}_2$ -dominated, but also exhibit a compositional diversity that reflects the complex processes (boiling, mixing and condensation) happening in the subsurface. In addition to  $\text{CO}_2$ , volcanic seeps are rich in reducing species ( $\text{H}_2\text{S}$ ,  $\text{CH}_4$ , and  $\text{H}_2$ ) whose ecological impacts and significance for future oceanic trends is currently poorly understood. In addition to the gas phase, volcanic seeps typically release a saline aqueous phase (brine) rich in a plethora

of trace elements of potentially significant biological importance. In the last decade, there has been a clear call for addressing the important effects of OA on high-level systems of life organization (i.e. biological communities and ecosystems), specifically when making predictions about the impacts of ongoing environmental change. We have shown recent advances in ecological research when using volcanic  $\text{CO}_2$  seeps as natural analogues for addressing ecosystem effects and winner and loser species under OA. Indeed, much progress has been made in designing ecological experiments along natural  $\text{CO}_2/\text{pH}$  gradients systems, however great caution is required to assess ecological responses in submarine seeps, especially when their geochemistry is unknown.

## Future directions

The study of the chemistry and ecology of volcanic  $\text{CO}_2$  seeps is an active field of research. Few shallow water submarine fields have been studied so far, and there is increasing need for a robust synthesis of this information, so future work should prioritize characterizing known (but unstudied) seeps, search for new ones, and assess how marine life acclimates or adapt to the high  $\text{CO}_2$  levels found at these sites. From a geochemical viewpoint,  $\text{CO}_2$  output estimates are available for only a few systems, and there is an opportunity to use newly developed technologies for in-situ, real-time mapping of  $\text{pCO}_2$  in seawater at high spatial and temporal resolution. From a biological point of view, progress is being made in our understanding of how coastal marine communities respond

to rising CO<sub>2</sub> levels. Over the next-decade CO<sub>2</sub> seep research efforts should characterize trace metal interactions with biological processes and make use of longer-term ecological experiments. Increased interaction and harmonization between geological, chemical and biological expertise looks set to provide improved insights into the responses of marine organisms to global OA.

**Funding** Open Access funding provided by Università degli Studi di Palermo. A.A. acknowledges funding support from the Alfred P. Sloan Foundation (Deep Carbon Observatory/DECADE project; UniPa-CiW subcontract 10881-1262) and the Italian Ministero Istruzione Università e Ricerca (MIUR, under Grant PRIN2017-2017LMNLAW).

**Data availability** All data used in the manuscript are contained in the associated Supplementary Materials.

### Compliance with ethical standards

**Conflict of interest** The authors declare no conflict of interest.

**Open Access** This article is licensed under a Creative Commons Attribution 4.0 International License, which permits use, sharing, adaptation, distribution and reproduction in any medium or format, as long as you give appropriate credit to the original author(s) and the source, provide a link to the Creative Commons licence, and indicate if changes were made. The images or other third party material in this article are included in the article's Creative Commons licence, unless indicated otherwise in a credit line to the material. If material is not included in the article's Creative Commons licence and your intended use is not permitted by statutory regulation or exceeds the permitted use, you will need to obtain permission directly from the copyright holder. To view a copy of this licence, visit <http://creativecommons.org/licenses/by/4.0/>.

### References

- Agostini A, Harvey BP, Wada S, Kon K, Milazzo M, Inaba K, Hall-Spencer JM (2018) Ocean acidification drives community shifts towards simplified non-calcified habitats in a subtropical–temperate transition zone. *Sci Rep* 8:11354. <https://doi.org/10.1038/s41598-018-29251-7>
- Albright R, Takeshita Y, Koweek D, Ninokawa A, Wolfe K, Rivlin T, Nebuchina Y, Young J, Caldeira K (2018) Carbon dioxide addition to coral reef waters suppresses net community calcification. *Nature* 555:516–519. <https://doi.org/10.1038/nature25968>
- Alessi C, Giomi F, Furnari F, Sarà G, Chemello R, Milazzo M (2019) Ocean acidification and elevated temperature negatively affect recruitment, oxygen consumption and calcification of the reef-building *Dendropoma cristatum* early life stages: evidence from a manipulative field study. *Sci Total Environ* 693:133476. <https://doi.org/10.1016/j.scitotenv.2019.07.282>
- Alt JC (1995) Seafloor processes in mid-ocean ridge hydrothermal systems. In: Humphris SE, Zierenberg RA, Mullineaux LS, Thomson RE (eds) Seafloor hydrothermal systems: physical, chemical, biological, and geological interactions. American Geophysical Union, Washington, D.C., pp 85–114
- Apostolaki ET, Vizzini S, Hendriks IE, Olsen YS (2014) Seagrass ecosystem response to long-term high CO<sub>2</sub> in a Mediterranean volcanic vent. *Mar Environ Res* 99:9–15
- Baross JA, Hoffman SE (1985) Submarine hydrothermal vents and associated gradient environments as sites for the origin and evolution of life. *Origins Life* 15:327–345
- Becke R, Merkel B, Pohl T (2009) Mineralogical and geological characteristics of the shallow-water massive sulfide precipitates of Panarea, Aeolian Islands, Italy. In: Merkel B, Schipek M (eds) Research in shallow marine and fresh water systems. Freiberg online geology. TU Bergakademie, Freiberg, pp 94–100
- Boatta F, D'Alessandro W, Gagliano AL, Liotta M, Milazzo M, Rodolfo-Metalpa R, Hall-Spencer JM, Parello F (2013) Geochemical survey of Levante Bay, Vulcano Island (Italy), a natural laboratory for the study of ocean acidification. *Mar Pollut Bull* 73:485–494
- Brinkman TJ (2014) Suitability of volcanic vents at White Island, New Zealand for climate change research: effects on sea urchins and coralline algae (Doctoral dissertation, University of Otago)
- Brodie J, Williamson CJ, Smale DA, Kamenos NA, Mieszkowska N, Santos R et al (2014) The future of the northeast Atlantic benthic flora in a high CO<sub>2</sub> world. *Ecol Evol* 4:2787–2798. <https://doi.org/10.1002/ece3.1105>
- Brown NEM, Milazzo M, Rastrick SPS, Hall-Spencer JM, Therriault TW, Harley CGD (2018) Natural acidification changes the timing and rate of succession, alters community structure, and increases homogeneity in marine biofouling communities. *Glob Change Biol* 24(1):112–127. <https://doi.org/10.1111/gcb.13856>
- Butterfield A, Massoth GJ, McDuff RE, Lupton JE, Lilley MD (1990) Geochemistry of hydrothermal fluids from Axial Seamount hydrothermal emissions study vent field, Juan de Fuca Ridge: seafloor boiling and subsequent fluid–rock interaction. *J Geophys Res* 95:12895–12921
- Caliro S, Caracausi A, Chiodini G, Ditta M, Italiano F, Longo M, Minopoli C, Nuccio PM, Rizzo A (2004) Evidence of a new magmatic input to the quiescent volcanic edifice of Panarea, Aeolian Islands, Italy. *Geophys Res Lett* 31:1–5
- Calosi P, Rastrick SPS, Graziano M, Thomas SC, Baggini C, Carter HA, Hall-Spencer J, Milazzo M, Spicer JJ (2013) Acid-base and ion-regulation capacity-dependent distribution of sea urchins living near shallow water CO<sub>2</sub> vents. *Mar Pollut Bull* 73:470–484. <https://doi.org/10.1016/j.marpolbul.2012.11.040>
- Camp EF, Schoepf V, Mumby PJ, Hardtke LA, Rodolfo-Metalpa R, Smith DJ, Suggett DJ (2018) The future of coral reefs subject to rapid climate change: lessons from natural extreme environments. *Front Mar Sci* 5:4. <https://doi.org/10.3389/fmars.2018.00004>
- Capaccioni B, Tassi F, Vaselli O (2001) Organic and inorganic geochemistry of low temperature gas discharges at the Baia

- di Levante beach, Vulcano Island, Italy. *J Volcanol Geotherm Res* 108:173–185
- Capasso G, Inguaggiato S (1998) A simple method for the determination of dissolved gases in natural waters. An application to thermal waters from Vulcano Island. *Appl Geochem* 13(5):631–642
- Caracausi A, Ditta M, Italiano F, Longo M, Nuccio PM, Paonita A (2005) Massive submarine gas output during the volcanic unrest off Panarea Island (Aeolian arc, Italy): inferences for explosive conditions. *Geochem J* 39:459–467
- Cattano C, Claudet J, Domenici P, Milazzo M (2018) Living in a high CO<sub>2</sub> world: a global meta-analysis shows multiple trait-mediated fish responses to ocean acidification. *Ecol Monogr* 88(3):320–335. <https://doi.org/10.1002/ecm.1297>
- Cattano C, Agostini S, Harvey BP, Wada S, Quattrocchi F, Turco G, Inaba K, Hall-Spencer JM, Milazzo M (2020) Changes in fish communities due to benthic habitat shifts under ocean acidification conditions. *Sci Total Environ* 725:138501. <https://doi.org/10.1016/j.scitotenv.2020.138501>
- Chen XG, Zhang HY, Xiaohu L, Chen C-TA (2016) The chemical and isotopic compositions of gas discharge from shallow-water hydrothermal vents at Kueishantao, offshore northeast Taiwan. *Geochem J* 50:341–355
- Chiodini G, Marini L (1998) Hydrothermal gas equilibria: the H<sub>2</sub>O-H<sub>2</sub>-CO<sub>2</sub>-CO-CH<sub>4</sub> system. *Geochim Cosmochim Acta* 62:2673–2687
- Chiodini G, Cioni R, Marini L (1993) Reactions governing the chemistry of crater fumaroles from Vulcano Island Italy, and implications for volcanic surveillance. *Appl Geochem* 8:357–371
- Chiodini G, Cioni R, Marini L, Panichi C (1995) Origin of fumarolic fluids of Vulcano Island Italy and implications for volcanic surveillance. *Bull Volcanol* 57:99–110
- Connell SD, Doubleday ZA, Hamlyn SB, Foster NR, Harley CDG, Kelaher BP, Nagelkerken I, Sara G, Russell BD (2017) How ocean acidification can benefit calcifiers. *Curr Biol* 27:R95–R96
- Connell SD, Doubleday ZA, Foster NR, Hamlyn SB, Harley CDG, Helmuth B, Kelaher BP, Nagelkerken I, Rodgers KL, Sarà G, Russell BD (2018) The duality of ocean acidification as a resource and a stressor. *Ecology* 88:1005–1010
- Cornwall CE, Revill AT, Hall-Spencer JM, Milazzo M, Raven JA, Hurd CL (2017) Inorganic carbon physiology underpins macroalgal responses to elevated CO<sub>2</sub>. *Sci Rep* 7:46297
- Cornwall CE, Comeau S, DeCarlo TM, Larcombe E, Moore B, Giltrow K et al (2020) A coralline alga gains tolerance to ocean acidification over multiple generations of exposure. *Nat Clim Change* 10:149
- Crook ED, Kroeker KJ, Potts DC, Rebolledo-Vieyra M, Hernandez-Terrones LM, Paytan A (2016) Recruitment and succession in a tropical benthic community in response to in-situ ocean acidification. *PLoS ONE* 11(1):e0146707
- Dando PR (2010) Biological communities at marine shallow-water vent and seep sites. In: Kiel S (ed) *The vent and seep biota topics in geobiology*. Springer, New York
- de Ronde CEJ, Stucker VK (2015) Seafloor hydrothermal venting at volcanic arcs and Backarcs, *Encyclopaedia of volcanoes*, 2nd edn. Elsevier, Hoboken, pp 823–849
- Di Napoli R et al (2016) Hydrothermal fluid venting in the offshore sector of Campi Flegrei caldera: a geochemical, geophysical, and volcanological study. *Geochem Geophys Geosyst*. <https://doi.org/10.1002/2016GC006494>
- Doney SC, Busch DS, Cooley SR, Kroeker KJ (2020) The impacts of ocean acidification on marine ecosystems and reliant human communities. *Annu Rev Environ Resour* 45:83–112
- Donnarumma L et al (2019) Environmental and benthic community patterns of the shallow hydrothermal area of Secca delle Fumose (Baia, Naples, Italy). *Front Mar Sci* 6:685. <https://doi.org/10.3389/fmars.2019.00685>
- Ekstrom JA et al (2015) Vulnerability and adaptation of US shellfisheries to ocean acidification. *Nat Clim Change* 5(3):207
- Enochs IC, Manzello DP, Donham EM, Kolodziej G, Okano R, Johnston L, Young C, Iguel J, Edwards CB, Fox MD, Valentino L, Johnson S, Benavente D, Clark SJ, Carlton R, Burton T, Eynaud Y, Price NN (2015) Shift from coral to macroalgae dominance on a volcanically acidified reef. *Nat Clim Change* 5:1083–1088. <https://doi.org/10.1038/nclimate2758>
- Fabricius KE, Langdon C, Uthicke S, Humphrey C, Noonan S, De'ath G, Okasaki R, Muehllehner N, Glas MS, Lough JM (2011) Losers and winners in coral reefs acclimated to elevated carbon dioxide concentrations. *Nat Clim Change* 1:165–169. <https://doi.org/10.1038/nclimate1122>
- Fabricius KE, De'ath G, Noonan S, Uthicke S (2014) Ecological effects of ocean acidification and habitat complexity on reef-associated macroinvertebrate communities. *Proc R Soc B* 281(1775):20132479. <https://doi.org/10.1098/rspb.2013.2479>
- Fabricius KE, Kluebenschedl A, Harrington L, Noonan S, De'ath G (2015) In situ changes of tropical crustose coralline algae along carbon dioxide gradients. *Sci Rep* 5:9537. <https://doi.org/10.1038/srep09537>
- Fietzek P, Fiedler B, Steinhoff T, Körtzinger A (2014) In situ quality assessment of a novel underwater pCO<sub>2</sub> sensor based on membrane equilibration and NDIR Spectrometry. *J Atmos Oceanic Technol* 31:181–196. <https://doi.org/10.1175/JTECH-D-13-00083.1>
- Fischer TP, Chiodini G (2015) Volcanic, magmatic and hydrothermal gas discharges. *Encyclopaedia of volcanoes*, 2nd edn. Elsevier, Hoboken, pp 779–797
- Foo SA, Byrne M, Ricevuto E, Gambi MC (2018) Oceanography and marine biology: an annual review. *Oceanogr Mar Biol* 56:237–310
- Foster GL, Royer DL, Lunt DJ (2017) Future climate forcing potentially without precedent in the last 420 million years. *Nat Commun* 8:14845. <https://doi.org/10.1038/ncomms14845>
- Foustoukos DI, Seyfried WE (2007) Fluid phase separation processes in submarine hydrothermal systems. *Rev Miner Geochem* 65:213–239
- Garilli V, Rodolfo-Metalpa R, Scuderi D, Brusca L, Parrinello D, Rastrick SPS, Foggo A, Twitchett RJ, Hall-Spencer JM, Milazzo M (2015) Physiological advantages of dwarfing in surviving extinctions in high-CO<sub>2</sub> oceans. *Nat Clim Change* 5:678–682. <https://doi.org/10.1038/nclimate2616>
- Garrard SL, Gambi MC, Scipione MB, Patti FP, Lorenti M, Zupo V, Paterson DM, Buia MC (2014) Indirect effects

- may buffer negative responses of seagrass invertebrate communities to ocean acidification. *J Exp Mar Biol Ecol* 461:31–38
- Gaylord B, Kroeker KJ, Sunday JM, Anderson KM, Barry JP, Brown NE, Connell SD, Dupont S, Fabricius KE, Hall-Spencer JM, Klinger T, Milazzo M, Munday PL, Russell BD, Sanford E, Schreiber SJ, Thiyagarajan V, Vaughan MLH, Widdicombe S, Harley CDG (2015) Ocean acidification through the lens of ecological theory. *Ecology* 96:3–15. <https://doi.org/10.1890/14-0802.1>
- German CR, Von Damm KL (2003) Hydrothermal processes. In: Turekian KK, Holland HD (eds) *Treatise on geochemistry*. Elsevier, Boboken, pp 145–180
- Global CCS institute (2018) CCS Facilities Database. <https://www.globalccsinstitute.com/resources/ccs-database-public/>. Accessed 2 Apr 2019
- Giggenbach WF (1980) Geothermal gas equilibria. *Geochim Cosmochim Acta* 44:2021–2032
- Giggenbach WF (1987) Redox processes governing the chemistry of fumarolic gas discharges from White Island, New Zealand. *Appl Geochem* 2:143–161
- Giggenbach WF (1988) Geothermal solute equilibria. Derivation of Na–K–Mg–Ca geothermometers. *Geochim et Cosmochim Acta* 52(12):2749–2765
- Giggenbach WF (1997) The origin and evolution of fluids in magmatic hydrothermal systems. In: Barnes HL (ed) *Geochemistry of hydrothermal ore deposits*, 3rd edn. Wiley, New York, pp 699–736
- Goffredo S, Prada F, Caroselli E, Capaccioni B, Zaccanti F, Pasquini L, Fantazzini P, Fermani S, Reggi M, Levy O, Fabricius K, Dubinsky Z, Falini G (2014) Biomineralization control related to population density under ocean acidification. *Nat Clim Change* 4:593–597
- González-Delgado S, Hernández JC (2018) The importance of natural acidified systems in the study of ocean acidification: what have we learned? *Adv Mar Biol*. <https://doi.org/10.1016/bs.amb.2018.08.001>
- Hall-Spencer JM, Rodolfo-Metalpa R, Martin S, Ransome E, Fine M, Turner SM, Rowley SJ, Tedesco D, Buia MC (2008) Volcanic carbon dioxide vents show ecosystem effects of ocean acidification. *Nature* 454:96–99. <https://doi.org/10.1038/nature07051>
- Hall-Spencer JM, Allen R (2015) The impact of CO<sub>2</sub> emissions on ‘nuisance’ marine species. *Res Rep Biodivers Stud* 4:33–46
- Hall-Spencer JM, Harvey BP (2019) Ocean acidification impacts on coastal ecosystem services due to habitat degradation. *Emerg Top Life Sci* 3(2):197–206
- Hannington MD, de Ronde CEJ, Petersen S (2005) Modern seafloor tectonics and submarine hydrothermal systems. *Econ Geol* 100:111–141
- Hannington M, Jamieson J, Monecke T, Petersen S, Beaulieu S (2011) The abundance of seafloor massive sulfide deposits. *Geology* 39–12:1155–1158. <https://doi.org/10.1130/G32468.1>
- Harvey BP, Gwynn-Jones D, Moore PJ (2013) Meta-analysis reveals complex marine biological responses to the interactive effects of ocean acidification and warming. *Ecol Evol* 3(4):1016–1030
- Harvey BP, Agostini S, Kon K, Wada S, Hall-Spencer JM (2019) Diatoms dominate and alter marine food-webs when CO<sub>2</sub> rises. *Diversity* 11(12):242
- Harvey BP, McKeown NJ, Rastrick PS, Bertolini C, Foggo A, Graham H, Hall-Spencer JM, Milazzo M, Shaw PW, Small DP, Moore PJ (2016) Individual and population-level responses to ocean acidification. *Sci Rep* 4:20194. <https://doi.org/10.1038/srep20194>
- Hedenquist JW, Lowenstern JB (1994) The role of magmas in the formation of hydrothermal ore deposits. *Nature* 370:519–527
- Hedges LV, Gurevitch J, Curtis PS (1999) The meta-analysis of response ratios in experimental ecology. *Ecology* 80:1150–1156
- Hendriks IE, Duarte CM, Alvarez M (2010) Vulnerability of marine biodiversity to ocean acidification: a meta-analysis. *Estuar Coast Shelf S* 86(2):157–164
- Hesselbo SP, Gröcke DR, Jenkyns HC, Bjerrum CJ, Farrimond P, Morgans Bell HS, Green OR (2000) Massive dissociation of gas hydrate during a Jurassic oceanic anoxic event. *Nature* 406:392–395. <https://doi.org/10.1038/35019044>
- Kroeker K, Kordas RL, Crim RN, Singh GG (2010) Meta-analysis reveals negative yet variable effects of ocean acidification on marine organisms. *Ecol Lett* 13:1419–1434
- Kroeker KJ, Micheli F, Gambi MC, Martz TR (2011) Divergent ecosystem responses within a benthic marine community to ocean acidification. *Proc Natl Acad Sci USA* 108:14515–14520. <https://doi.org/10.1073/pnas.1107789108>
- Kroeker KJ, Kordas RL, Crim R, Hendriks IE, Ramajo L, Singh GS, Duarte CM, Gattuso JP (2013) Impacts of ocean acidification on marine organisms quantifying sensitivities and interaction with warming. *Glob Change Biol* 19:1884–1896. <https://doi.org/10.1111/gcb.12179>
- IPCC (2019) Special report on the ocean and cryosphere in a changing climate. <https://www.ipcc.ch/srocc/>
- Inguaggiato S, Mazot A, Diliberto IS, Inguaggiato C, Madonia P, Rouwet D, Vita F (2012) Total CO<sub>2</sub> output from Vulcano island (Aeolian Islands, Italy). *Geochem Geophys Geosyst* 13(2):Q02012
- Inoue S, Kayanne H, Yamamoto S, Kurihara H (2013) Spatial community shift from hard to soft corals in acidified water. *Nat Clim Change* 3:683–687. <https://doi.org/10.1038/nclimate1855>
- Italiano F (2009) Hydrothermal fluids vented at shallow depths at the Aeolian islands: relationships with volcanic and geothermal systems. *Freiberg Online Geol* 22:55–60
- Italiano F, Nuccio PM (1991) Geochemical investigation of submarine volcanic exhalations to the east of Panarea, Aeolian Island, Italy. *J Volcanol Geotherm Res* 46:125–141
- Italiano F, Nuccio PM, Sommaruga C (1984) Gas/steam and thermal energy release measured at the gaseous emissions of the Baia di Levante of Vulcano Island, Italy. *Acta Vulcanol* 5:89–94
- Italiano F, Nuccio PM, Pecoraino G (1994) Fumarolic gas output at La Fossa di Vulcano crater. *Acta Vulcanol* 6:39–40
- Jenkyns HC (2003) Evidence for rapid climate change in the Mesozoic-Palaeogene greenhouse world. *Philos Trans R*

- Soc Lond Ser A 361:1885–1916. <https://doi.org/10.1098/rsta.2003.1240>
- Jenkyns HC (2010) Geochemistry of ocean anoxic events. *Geochem Geophys Geosyst* 11:3. <https://doi.org/10.1029/2009GC002788>
- Johnson VR, Brownlee C, Rickaby REM, Graziano M, Milazzo M, Hall-Spencer JM (2013) Responses of marine benthic microalgae to elevated CO<sub>2</sub>. *Mar Biol* 160:1813–1824. <https://doi.org/10.1007/s00227-011-1840-2>
- Lam VWY, Chavanich S, Djoundourian S, Dupont S, Gail F, Holzer G, Isensee K, Katua S, Mars F, Metian M, Hall-Spencer JM (2019) Dealing with the effects of ocean acidification on coral reefs in the Indian Ocean and Asia. *Region Stud Mar Sci* 28:100560
- Lemasson AJ, Hall-Spencer JM, Kuri V, Knights AM (2019) Changes in the biochemical and nutrient composition of seafood due to ocean acidification and warming. *Mar Environ Res* 143:82–92. <https://doi.org/10.1016/j.marenvres.2018.11.006>
- Linares C, Vidal M, Canals M, Kersting DK, Amblas D, Aspillaga E, Cebrián E, Delgado-Huertas A, Díaz D, Garrabou J, Hereu B, Navarro L, Teixidó N, Ballesteros E (2015) Persistent natural acidification drives major distribution shifts in marine benthic ecosystems. *Proc R Soc B* 282:e20150587. <https://doi.org/10.1098/rspb.2015.0587>
- Lu G-S, LaRowe DE, Fike DA, DruschelGK GWP III, Price RE et al (2020) Bioenergetic characterization of a shallow-sea hydrothermal vent system: Milos Island, Greece. *PLoS ONE* 15(6):e0234175. <https://doi.org/10.1371/journal.pone.0234175>
- Lupton J, De Ronde C, Sprovieri M, Baker ET, Bruno PP, Italiano F, Walker S, Faure K, Leybourne M, Britten K, Greene R (2011) Active hydrothermal discharge on the submarine Aeolian Arc. *J Geophys Res* 116(2):B02102. <https://doi.org/10.1029/2010JB007738>
- Martin S, Rodolfo-Metalpa R, Ransome E, Rowley S, Buia M-C, Gattuso J-P, Hall-Spencer JM (2008) Effects of naturally acidified seawater on seagrass calcareous epibionts. *Biol Lett* 4:689–692
- Martins M, Carreiro-Silva M, Martins GM, Barcelos e Ramos J, Viveiros F, Couto R, Parra H, Monteiro J, Gallo F, Silva C, Teodósio A, Guilini K, Hall-Spencer JM, Leitão F, Chícharo L, Range P (2020) *Ervilia castanea* (Mollusca, Bivalvia) populations adversely affected at CO<sub>2</sub> seeps in the North Atlantic. *Sci Total Environ* 754:142044
- Marty B, Alexander CMO, Raymond SN (2013) Primordial origins of earth's carbon. *Rev Miner Geochem* 75:149–181. <https://doi.org/10.2138/rmg.2013.75.6>
- Meyer KM, Kump LR (2008) Oceanic euxinia in Earth history: causes and consequences. *Ann Rev Earth Planet Sci* 36:251–288
- Micheli F, Halpern BS (2005) Low functional redundancy in coastal marine assemblages. *Ecol Lett* 8(4):391–400. <https://doi.org/10.1111/j.1461-0248.2005.00731.x>
- Milazzo M, Rodolfo-Metalpa R, San Chan VB, Fine M, Alessi C, Thiagarajan V, Hall-Spencer JM, Chemello R (2014) Ocean acidification impairs vermetid reef recruitment. *Sci Rep* 4:4189. <https://doi.org/10.1038/srep04189>
- Milazzo M, Alessi C, Quattrocchi F, Chemello R, D'Agostaro R, Gil J, Vaccaro AM, Mirto S, Gristina M, Badalamenti F (2019) Biogenic habitat shifts under long-term ocean acidification show nonlinear community responses and unbalanced functions of associated invertebrates. *Sci Total Environ* 667:41–48. <https://doi.org/10.1016/j.scitotenv.2019.02.39>
- Mishra AK, Santos R, Hall-Spencer JM (2020) Elevated trace elements in sediments and seagrasses at CO<sub>2</sub> seeps. *Mar Environ Res*. <https://doi.org/10.1016/j.marenvres.2019.104810>
- Nagelkerken I, Russell BD, Gillanders BM, Connell SD (2015) Ocean acidification alters fish populations indirectly through habitat modification. *Nat Clim Change* 6:89–93
- Paonita A, Federico C, Bonfanti P, Capasso G, Inguaggiato S, Italiano F, Madonia P, Pecoraino G, Sortino F (2013) The episodic and abrupt geochemical changes at La Fossa fumaroles (Vulcano Island, Italy) and related constraints on the dynamics, structure, and compositions of the magmatic system. *Geochim Cosmochim Acta* 120:158–178. <https://doi.org/10.1016/j.gca.2013.06.015>
- Pichler T, Veizer J (1999) Precipitation of Fe(III) oxyhydroxide deposits from shallowwaterhydrothermal fluids in Tutum Bay, Ambitle Island, Papua New Guinea. *Chem Geol* 162:15–31. [https://doi.org/10.1016/S0009-2541\(99\)00068-6](https://doi.org/10.1016/S0009-2541(99)00068-6)
- Pichler T, Veizer J, Hall GEM (1999a) The chemical composition of shallow-water hydrothermal fluids in Tutum Bay, Ambitle Island, Papua New Guinea and their effect on ambient seawater. *Mar Chem* 64(3):229–252
- Pichler T, Veizer J, Hall GEM (1999b) The natural input of extremely high arsenic concentrations into a coral reef ecosystem by hydrothermal fluids and its removal by Fe(III) oxyhydroxides. *Environ Sci Technol* 33:1373–1378
- Pichler T, Biscéré T, Kinch J, Zampighi M, Houlbrèque F, Rodolfo-Metalpa R (2019) Suitability of the shallow water hydrothermal system at Ambitle Island (Papua New Guinea) to study the effect of high pCO<sub>2</sub> on coral reefs. *Mar Pollut Bull* 138:148–158
- Price RE, Giovannelli D (2017) A review of the geochemistry and microbiology of marine shallow-water hydrothermal vents. *Ref Module Earth Syst Environ Sci*. <https://doi.org/10.1016/B978-0-12-409548-9.09523-3>
- Price RE, Pichler T (2005) Distribution, speciation and bioavailability of arsenic in ashallow-water submarine hydrothermal system, Tutum Bay, Ambitle Island, PNG. *Chem Geol* 224:122–135. <https://doi.org/10.1016/j.chemgeo.2005.07.017>
- Price RE, Savov I, Planer-Friedrich B, Buhning SI, Amend JP, Pichler T (2013) Processes influencing extreme As enrichment in shallow-sea hydrothermal fluids of Milos Island, Greece. *Chem Geol* 348:15–26. <https://doi.org/10.1016/j.chemgeo.2012.06.007>
- Price RE, LaRowe DE, Italiano F, Savov I, Pichler T, Amend JP (2015) Subsurface hydrothermal processes and the bioenergetics of chemolithoautotrophy at the shallow-sea vents off Panarea Island (Italy). *Chem Geol* 407:21–45. <https://doi.org/10.1016/j.chemgeo.2015.04.011>
- Porzio L, Buia MC, Hall-Spencer JM (2011) Effects of ocean acidification on macroalgal communities. *J Exp Mar Biol Ecol* 400:278–287
- Rainbow P (2002) Trace metal concentrations in aquatic invertebrates: why and so what? *Environ Pollut* 120:497–507. [https://doi.org/10.1016/S0269-7491\(02\)00238-5](https://doi.org/10.1016/S0269-7491(02)00238-5)

- Rastrick SSP, Graham H, Azetsu-Scott K, Calosi P, Chierici M, Fransson A, Hop H, Hall-Spencer JM, Milazzo M, Thor P, Kutti T (2018) Using natural analogues to investigate the effects of climate change and ocean acidification on Northern ecosystems. *ICES J Mar Sci* 75:2299–2311. <https://doi.org/10.1093/icesjms/fsy128>
- Riebesell U, Gattuso J-P (2015) Lessons learned from ocean acidification research. *Nat Clim Change* 5:12–14. <https://doi.org/10.1038/nclimate2456>
- Royer DL, Berner RA, Park J (2007) Climate sensitivity constrained by CO<sub>2</sub> concentrations over the past 420 million years. *Nature* 446:530–532
- Russell BD, Connell SD, Uthicke S, Muehlllehner N, Fabricius KE, Hall-Spencer JM (2013) Future seagrass beds: can increased productivity lead to increased carbon storage? *Mar Pollut Bull* 73(2):463–469. <https://doi.org/10.1016/j.marpolbul.2013.01.031>
- Sedwick P, Stuben D (1996) Chemistry of shallow submarine warm springs in an arc-volcanic setting: Vulcano Island, Aeolian Archipelago, Italy. *Mar Chem* 53:147–161
- Shamberger KEF, Cohen AL, Golbuu Y, McCorkle DC, Lentz SJ, Barkley HC (2014) Diverse coral communities in naturally acidified waters of a Western Pacific Reef. *Geophys Res Lett* 41:499–504. <https://doi.org/10.1002/2013GL058489>
- Sommaruga C (1984) Le ricerche geotermiche svolte a Vulcano negli anni '50. *Rend Soc Ital Miner Petrol* 39:355–366
- Stumm W, Morgan JJ (1995) Aquatic chemistry: chemical equilibria and rates in natural waters, 3rd edn. Wiley, Hoboken
- Suggett DJ, Hall-Spencer JM, Rodolfo-Metalpa R, Boatman TG, Payton R, Tye Pettay D, Johnson VR, Warner ME, Lawson T (2012) Sea anemones may thrive in a high CO<sub>2</sub> world. *Glob Change Biol* 18:3015–3025
- Sunday JM, Fabricius KE, Kroeker KJ, Anderson KM, Brown NE, Barry JP, Connell SD, Dupont S, Gaylord B, Hall-Spencer JM, Klinger T, Milazzo M, Munday PL, Russell BD, Sanford E, Thiagarajan V, Vaughan MLH, Widdicombe S, Harley CDG (2017) Ocean acidification can mediate biodiversity shifts by changing biogenic habitat. *Nat Clim Change* 7:81–85. <https://doi.org/10.1038/nclimate3161>
- Tarasov VG, Gebruk AV, Mironov AN, Moskalev LI (2005) Deep-sea and shallow-water hydrothermal vent communities: two different phenomena? *Chem Geol* 224:5–39
- Tedesco D (1995) Fluid geochemistry at Vulcano Island: a change in the volcanic regime or continuous fluctuations in the mixing of different systems? *J Geophys Res* 100(B3):4157–4167
- Teixidó N, Gambi MC, Parravacini V, Kroeker K, Micheli F, Ballesteros E (2018) Functional biodiversity loss along natural CO<sub>2</sub> gradients. *Nat Commun* 9:5149
- Thomsen J, Gutowska MA, Saphörster J, Heinemann A, Trübenbach K, Fietzke J, Hiebenthal C, Eisenhauer A, Körtzinger A, Wahl M, Melzner F (2010) Calcifying invertebrates succeed in a naturally CO<sub>2</sub>-rich coastal habitat but are threatened by high levels of future acidification. *Biogeosciences* 7:3879–3891. <https://doi.org/10.5194/bg-7-3879-2010>
- Tittensor DP, Baco-Taylor AR, Brewin P, Clark MR, Consalvey M, Hall-Spencer JM, Rowden AA, Schlacher T, Stocks K, Rogers AD (2009) Predicting global habitat suitability for stony corals on seamounts. *J Biogeogr* 36:1111–1128
- Tivey MK (2007) Generation of seafloor hydrothermal vent fluids and associated mineral deposits. *Oceanography* 20(1):50–65
- Tunnicliffe V (1991) The biology of hydrothermal vents: ecology and evolution. *Oceanogr Mar Biol Annu Rev* 29:3119–3207
- Turner LM, Ricevuto E, Massa-Gallucci A, Gambi MC, Calosi P (2015) Energy metabolism and cellular homeostasis trade-offs provide the basis for a new type of sensitivity to ocean acidification in a marine polychaete at a high-CO<sub>2</sub> vent: adenylate and phosphagen energy pools versus carbonic anhydrase. *J Exp Biol* 218:2148–2151
- Valsami-Jones E, Baltatzis E, Bailey EH, Boyce AJ, Alexander JL, Magganis A et al (2005) The geochemistry of fluids from an active shallow submarine hydrothermal system: Milos island, Hellenic Volcanic Arc. *J Volcanol Geotherm Res* 148(1–2):130–151
- Vizzini S, Di Leonardo R, Costa V, Tramati CDD, Luzzu F, Mazzola A (2013) Trace element bias in the use of CO<sub>2</sub> vents as analogues for low pH environments: implications for contamination levels in acidified oceans. *Estuar Coast Shelf Sci* 134:19–30
- Vizzini S, Martínez-Crego B, Andolina C, Massa-Gallucci A, Connell SD, Gambi MC (2017) Ocean acidification as a driver of community simplification via the collapse of higher-order and rise of lower-order consumers. *Sci Rep* 7:4018. <https://doi.org/10.1038/s41598-017-03802-w>
- Von Damm KL (1990) Seafloor hydrothermal activity: black smoker chemistry and chimneys. *Annu Rev Earth Planet Sci* 18:173–204. <https://doi.org/10.1146/annurev.earth.18.050190.001133>
- Von Damm KL, Lilley MD, Shanks WC, Brockington M, Bray AM, O'Grady KM, Olson E, Graham A, Proskurowski G (2003) Extraordinary phase separation and segregation in vent fluids from the southern East Pacific Rise. *Earth Planet Sci Lett* 206:365–378
- Wignall PB, Twitchett RJ (1996) Oceanic anoxia and the end-Permian mass extinction. *Science* 272:1155–1158
- Wignall PB, Twitchett RJ (2002) Extent, duration, and nature of the Permian-Triassic superanoxic event. *Geol Soc Am Spl Pap* 356:395–413
- Wittmann AC, Pörtner HO (2013) Sensitivities of extant animal taxa to ocean acidification. *Nat Clim Change* 3(11):995–1001
- Zitoun R et al (2020) A unique temperate rocky coastal hydrothermal vent system (Whakaari–White Island, Bay of Plenty, New Zealand): constraints for ocean acidification studies. *Mar Freshw Res* 71(3):321. <https://doi.org/10.1071/MF19167>
- Ziveri P, Passaro M, Incarbona A, Milazzo M, Rodolfo-Metalpa R, Hall-Spencer JM (2014) Decline in coccolithophore diversity and impact on coccolith morphogenesis along a natural CO<sub>2</sub> gradient. *Biol Bull* 226(3):282–290. <https://doi.org/10.1086/BBLv226n3p282>